REPUBLIC OF TURKEY

YILDIZ TECHNICAL UNIVERSITY

GRADUATE SCHOOL OF SCIENCE AND ENGINEERING

SYNTHESIS AND CHARACTERIZATION OF NANOPARTICLE INTEGRATED ANTIBACTERIAL CRYOGELS

Maria DAABOUL

MASTER OF SCIENCE THESIS

Department of Bioengineering

Bioengineering Program

Supervisor

Assoc. Prof. Dr. Murat TOPUZOĞULLARI

Co-Supervisor

Assoc. Prof. Dr. Mehmet Murat ÖZMEN

January 2023

REPUBLIC OF TURKEY

YILDIZ TECHNICAL UNIVERSITY

GRADUATE SCHOOL OF SCIENCE AND ENGINEERING

SYNTHESIS AND CHARACTERIZATION OF NANOPARTICLE INTEGRATED ANTIBACTERIAL CRYOGELS

A thesis submitted by Maria DAABOUL in partial fulfillment of the requirements for the degree of MASTER OF SCIENCE is approved by the committee on 09.01.2023 in Department of Bioengineering, Bioengineering Program.

Assoc. Prof. Dr. Murat TOPUZOĞULLARI Yıldız Technical University Supervisor	Assoc. Prof. Dr. Mehmet Murat ÖZMEN Yıldız Technical University Co- supervisor

Approved By the Examining Committee

Assoc. Prof. Dr. Murat TOPUZOĞULLARI, Supervisor
Yildiz Technical University _____

Prof. Dr. Suzan ABDURRAHMANOĞLU, Member
Marmara University _____

Assoc. Prof. Dr. Emrah Şefik ABAMOR, Member
Yildiz Technical University _____

I hereby declare that I have obtained the required legal permissions during data collection and exploitation procedures, that I have made the in-text citations and cited the references properly, that I haven't falsified and/or fabricated research data and results of the study and that I have abided by the principles of the scientific research and ethics during my Thesis Study under the title of Synthesis and Characterization of Nanoparticle Integrated Antibacterial Cryogels supervised by my supervisor, Assoc. Prof. Dr. Murat TOPUZOĞULLARI. In the case of a discovery of false statement, I am to acknowledge any legal consequence.

Maria DAABOUL

Signature

This study was supported by the Scientific Research Projects Coordination Unit of Yildiz Technical University. Project No: FCD-2022-4900.

Dedicated to everyone who contributed with their sincerest support

ACKNOWLEDGEMENTS

I would like to direct my dearest thanks to my supervisor; Assoc. Prof. Dr. Murat TOPUZOĞULLARI who guided and advocated me throughout the writing of this thesis alongside my co-supervisor; Assoc. Prof. Dr. Mehmet Murat ÖZMEN, who both presented their support in shaping this study to take its final form.

I would also like to present my gratitude to Assoc. Prof. Dr. Tülin ÖZBEK and her student Semra TAŞDURMAZLI from the Department of Molecular Biology and Genetics / Molecular Biology Laboratory consolidating this study.

Special thanks to Assoc. Prof. Dr. Emrah Şefik ABAMOR and PhD(c) Büşra Akgül from Cell Culture and Tissue Engineering Laboratory for all their support in the journey of bringing all theories into practice throughout the process of performing cytotoxicity tests.

Additional and immense thanks to Shifa ALHAMVİ, Eda Nur YETİŞKİN MORKAN, Hatice DEMİR, Damla GÖKKAYA ÖZBURUN and all the Biopolymer and Vaccine Laboratory (KMC306-307) personnel who contributed with sustained assistance.

I would also like to thank the Scientific Research Projects Coordination Unit of Yildiz Technical University for their support within the scope of the project numbered FCD-2022-4900.

Lastly, I would like to thank my family and friends for all their inputs and guidance both on the individual and professional side of this journey.

Maria DAABOUL

TABLE OF CONTENTS

LIST OF SYMBOLS

A	Absorbance
℃	Celsius Degree
cm	Centimeter
°	Degree
D	Diameter
Đ	Dispersity
q	Fraction
g	Gram
µg	Microgram
µL	Microliter
µm	Micrometer
mg	Milligram
mL	Milliliter
mmol	Milli-mole
mV	Millivolt
M	Molarity
MW	Molecular weight
nm	Nanometer
M_n	Number-average molecular weight
%	Percent
PdI	Polydispersity index
Q%	Quaternization degree
±	Standard Deviation
T	Transmittance
m	Weight
M_W	Weight-average molecular weight

LIST OF ABBREVIATIONS

^{1}H-NMR	Proton Nuclear Magnetic Resonance
4VP	4-Vinylpyridine
ACVA	4,4'-azobis(4-cyanovaleric acid)
Ag NPs	Silver Nanoparticles
AmPs	Antimicrobial Peptides
AMPS-Na	Sodium 2-acrylamido-2-methyl propyl sulfonate
APS	Ammonium Persulfate
BAAm	N,N'-Methylenebisacrylamide
CFU	Colony-Forming Units
DAPI	4′,6-diamidino-2-phenylindole
DLS	Dynamic Light Scattering
DMEM/F12	Dulbecco's Modified Eagle Medium
DMF	N,N'-Dimethylformamide
DMSO	Dimethyl Sulfoxide
E. coli	*Escherichia coli*
ECM	Extracellular Matrix
ELS	Electrophoretic Light Scattering
FBS	Fetal Bovine Serum
FDA	Food And Drug Administration
FTIR	Fourier-Transform Infrared Spectroscopy
GPC	Gel Permeation Chromatography
GTMAC	Glycidyl Trimethylammonium Chloride
HEMA	2-hydroxyethyl methacrylate

L929	Fibroblast cell line
MHB	Mueller-Hinton Broth
MTT	3-(4,5-dimethylthiazol-2yl)-2,5-diphenyltetrazolium bromide
NIPAM	Poly(N-isopropylacrylamide)
NPs	Nanoparticles
OEGMA-500	Poly(ethylene glycol) Methyl Ether Methacrylate (500)
PDA	Polydopamine
PEGMA	Poly(ethylene glycol) Methylether Methacrylate
PEI	Polyethyleneimine
PEO	Polyethylene Oxide
poly(HEMA-GMA)	poly(2-hydroxyethyl methacrylate-glycidyl methacrylate)
PVA	Poly(vinyl alcohol)
QP4VP	Quaternized Poly(4-vinylpyridine)
S.aureus	*Staphylococcus aureus*
SEM	Scanning Electron Microscope
TEMED	N,N,N′,N′-Tetramethyl Ethylenediamine
UV	Ultra-violet

LIST OF FIGURES

LIST OF TABLES

ABSTRACT

Synthesis and Characterization of Nanoparticle Integrated Antibacterial Cryogels

Maria DAABOUL

Department of Bioengineering

Master of Science Thesis

Supervisor: Assoc. Prof. Dr. Murat TOPUZOĞULLARI

Co- supervisor: Assoc. Prof. Dr. Mehmet Murat ÖZMEN

Cationic polymers are attracting attention as inherently antibacterial materials against antibiotic-resistant bacteria. These polymers are used in different forms, such as polymer-conjugates, nanoparticles, biofilms, and hydrogels, taking place in applications that require antibacterial activity. 4-vinylpyridine (4VP)-based polycations which have quaternary ammonium groups are good examples of such polymers.

Cryogels have found wide applications in many biomedical fields, including antibacterial studies, due to their open and interconnected porosity, super-fast swelling, and superior mechanical properties. In this study, 4VP and oligo(ethylene glycol) methyl ether methacrylate (OEGMA) cryogels with integrated 4VP-based cationic nanoparticles were produced. Poly(4VP-co-OEGMA) random copolymer was synthesized by free-radical polymerization of 4VP and OEGMA. The synthesized copolymer was cross-linked with a bifunctional agent by quaternization reaction to produce 4VP-based cationic nanoparticles. By attaching the synthesized nanoparticles to the pore wall surfaces of the cryogels

with quaternization reaction, nanoparticle-integrated, cationic, and inherently antibacterial cryogels were obtained. The produced copolymer, nanoparticles, and cryogels were characterized with FTIR, NMR, DLS/ELS spectroscopies, SEM and swelling tests. Moreover, the antibacterial activity of the cryogels against gram negative *(E. coli)* and gram positive *(S. aureus)* bacteria, and their biocompatibility on L929 mouse fibroblast cells were investigated in-vitro. The results showed that the produced cryogels exhibit super-fast swelling in less than one minute, average pore diameter of 50 μm, and the produced nanoparticles with hydrodynamic diameter of 112 $\pm$1 nm were attached to the pore gel walls successfully. The produced nanoparticle-integrated cryogels revealed antibacterial activity against both gram negative and gram positive bacteria and biocompatibility. In addition, the properties of nanoparticle-integrated cryogels were compared with bare and quaternized 4VP-OEGMA cryogels.

The produced biomaterials have the potential to be used in various biomedical applications, such as antibacterial surfaces, tissue engineering and wound dressings.

Keywords: Antibacterial, cryogel, nanoparticle, polycation, quaternization

ÖZET

Nanopartikül İçerikli Antibakteriyel Kriyojellerin Sentezi ve Karakterizasyonu

Maria DAABOUL

Biyomühendislik Anabilim Dalı

Yüksek Lisans Tezi

Danışman: Doç. Dr. Murat TOPUZOĞIULLARI

Eş-Danışman: Doç. Dr. Mehmet Murat ÖZMEN

Katyonik polimerler, antibiyotiğe dirençli bakterilere karşı kendiliğinden antibakteriyel malzemeler olarak dikkat çekmektedir. Bu polimerler, antibakteriyel aktivite gerektiren uygulamalarda yer alan polimer-konjugat, nanopartikül, biyofilm ve hidrojel gibi farklı yapılarda kullanılmaktadır. Kuarterner amonyum grubuna sahip 4-vinilpiridin (4VP)-esaslı polikatyonlar, bu tür polimerlere iyi örneklerdir.

Kriyojeller açık ve birbirleriyle bağlantılı gözeneklilik yapısı, süper hızlı şişme ve üstün mekanik özelliklerinden ötürü antibakteriyel çalışmalar dahil birçok biyomedikal alanda geniş bir uygulama alanı bulmuşlardır.

Bu çalışmada, yapısında 4VP-esaslı polimerik nanopartikül gömülü olan 4VP ve oligo (etilen glikol) metil eter metakrilat (OEGMA) esaslı kriyojeller üretilmiştir. Poli(4VP-ko-OEGMA) rastgele kopolimeri, 4VP ve OEGMA'nin serbest radikal polimerizasyonu ile sentezlenmiştir. Sentezlenen kopolimer, 4VP-esaslı katyonik nanopartiküller üretmek için iki-işlevli bir ajan ile kuarternizasyon reaksiyonu ile çapraz bağlanmıştır. Sentezlenen nanopartiküller kuarternizasyon reaksiyonu ile

kriyojellerin gözenek duvarı yüzeylerine tutturularak, nanopartikül gömülü, katyonik ve kendiliğinden antibakteriyel kriyojeller elde edilmiştir. Üretilen kopolimer, nanopartiküller ve kriyojeller FTIR, NMR, DLS/ELS spektroskopileri, SEM ve şişme testleri ile karakterize edilmiştir. Ayrıca sentezlenen kriyojellerin gram negatif *(E. coli)* ve gram pozitif *(S. aureus)* bakterilere karşı antibakteriyel aktivitesi ve L929 fare fibroblast hücreleri üzerindeki biyouyumluluğu in-vitro olarak incelenmiştir. Sonuçlar, sentezlenen kriyojellerin bir dakikadan kısa sürede süper hızlı şiştiğini, 50 μm boyutlarında gözenek çapına sahip olduklarını ve üretilen 112 ± 1 nm hidrodinamik çapa sahip nanopartiküllerin gözenek duvarlarına başarılı bir şekilde tutunmuş olduklarını göstermiştir. Üretilen nanopartikül-gömülü kriyojeller hem gram negatif hem de gram pozitif bakterilere karşı antibakteriyel aktivite göstermiş ve biyouyumluluk sergilemiştir. Ayrıca, nanopartikül gömülü kriyojellerin özellikleri, kuaternize edilmemiş ve kuaternize 4VP-OEGMA kriyojellerle karşılaştırılmıştır.

Üretilen biyomalzemeler; antibakteriyel yüzeyler, doku mühendisliği ve yara örtüleri gibi çeşitli biyomedikal uygulamalarda kullanılma potansiyeline sahip olduğu düşünülmektedir.

Anahtar Kelimeler: Antibakteriyel, kriyojel, kuarternizasyon, polikatyon, nanopartikül

1
INTRODUCTION

1.1 Literature Review

Bacterial infections occur generally when bacteria spread from tissues with a normal microbiota, such as the mucosal lining of nose and mouth, to areas with atypical colonization, such as the blood, kidney, and lung. Both long-term implants, such as joint implants, as well as temporary implants that connect between these two physiological areas, may aid with this bacterial translocation [1]. Moreover, bacterial resistance to current antibiotics is increasing rapidly [2] and the COVID-19 pandemic is expected to result in further increase in antibiotic resistance because of the high number of hospitalized patients taking antibiotics for the treatment of potential secondary infections[1], [3]. As a result, it is more crucial than ever to keep developing effective methods for treating bacterial infections with different action mechanisms from antibiotics to overcome this resistance [4]–[6].

Surface coatings and drug delivery systems with antibacterial activity have attracted interest in this field of study [5], [6]. Inherently antibacterial polymer-based biomaterials are promising alternatives that could help reduce concerns about resistance[7], [8]. These biomaterials can range from nano-scaled polymers [5] and nanoparticles [9] to macro-sized thin films and hydrogels [10]–[12].

Cryogels, which are macroporous hydrogels, are a great candidate in designing such antibacterial materials because of their macroporous structure, which enables them to be used while working with cells and biological molecules in addition to their high mechanical properties and super-fast swelling behavior [10], [13]. These materials can be synthesized from inherently antibacterial polymers, including polycations and antimicrobial polypeptides, or they can be functionalized by the integration of antibacterial agents to their structure, such as metallic nanoparticles or antibiotics. Antibacterial cryogels can be used in many applications [14], such as surface coating, tissue engineering [15], wound

dressing [16] and water treatment [17]. As a result, efforts are being made to develop antibacterial cryogels.

Quaternary vinylpyridine polymers are examples of inherently antibacterial polycations that have high antibacterial activity but also have cytotoxic effects. For this reason, their biocompatibility can be increased with the addition of biocompatible, hydrophilic monomers, such as oligo(ethylene glycol) methyl ether methacrylate (OEGMA).

In literature, several antibacterial cryogels prepared from different polymers are found. İşoğlu et al. produced poly(4VP) and hydroxypropyl methacrylamide (HPMA) based double-layered wound dressing cryogels for wounds with high risk of infection. In addition, ascorbic acid (vitamin C) was loaded to the cryogel layer to improve the healing mechanism. These materials are designed to protect the wound from secondary infections where the synthesized biomaterial showed antibacterial and antifungal activity against *Staphylococcus aureus* and *Candida albicans*, respectively [18].

Integrating antibacterial nanoparticles to the cryogels is an effective method to prepare antibacterial materials. Silver nanoparticle is the most commonly used nanoparticle in such biomaterials [19]–[22]. For instance, chitosan-based cryogels were prepared from gelatin/chitosan/silver nanoparticle composites with tannic acid as a cross-linker. In this study, silver nanoparticle-embedded chitosan cryogels with gelatin as a stabilizer were synthesized. The addition of silver nanoparticles showed enhancement in the mechanical and swelling properties of the cryogels. The produced biomaterial showed biocompatibility and antibacterial activity, in addition to prompting in-vivo wound healing [23].

Antibacterial polymeric nanoparticles can also be integrated into cryogel structure to obtain antibacterial materials. The study of Sahiner et al. is the only study in which inherently antibacterial polymeric nanoparticles are integrated in the structure of cryogels. Sahiner et al. have prepared poly(tannic acid) (poly(TA) macro-, micro- and nanoparticles and embedded them in poly(2-hydroxyethyl methacrylate) (poly(HEMA)) cryogels. The cryogel provided pH-sensitive controlled release of the polymeric particles and was demonstrated as wound

dressing biomaterial. The introduction of poly(TA) particles into the supermacroporous poly(HEMA) cryogels gave additional capabilities like antioxidant and antibacterial activities due to the intrinsic qualities of TA. Additionally, poly(TA) particle-embedded poly(HEMA) cryogel composites had rapid swelling, high moisture content, strong hemocompatibility, high hemostatic characteristics, and the capacity to cause blood clotting, making them excellent candidates for use as wound dressing materials [24].

Although there are several antibacterial agent-integrated macroporous hydrogels, the number of studies in which polymeric nanoparticles are integrated is very limited. From this point, 4VP and OEGMA monomers-based cationic nanoparticle-integrated antibacterial cryogels were produced in this study for the first time in literature. In addition, 4VP-OEGMA based antibacterial cryogels were synthesized for the first time in this study.

1.2 Objective of the Thesis

The aim of this study is to produce polymeric nanoparticle-integrated antibacterial cryogels using 4VP and OEGMA monomers. In this study, the effect of the quaternization and polymeric antibacterial nanoparticle integration on the features and antibacterial activity against gram negative (*E. coli*) and gram positive (*S. aureus*) bacteria of the synthesized 4VP-OEGMA cryogels were investigated.

To achieve this purpose,

- The synthesis of poly(4VP-co-OEGMA) random copolymer by free-radical polymerization of 4VP and OEGMA monomers,
- Cross-linking the produced copolymer with bi-functional agent to prepare 4VP-based cationic nanoparticles,
- The synthesis of 4VP-OEGMA cryogels by cryogelation of 4VP and OEGMA monomers with free-radical polymerization,
- The quaternization of the prepared cryogels with alkylating agent through quaternization reaction,
- The integration of the produced antibacterial nanoparticles to the prepared non-quaternized cryogels by quaternization reaction, and

- The investigation of the antibacterial activity of the produced cryogels against gram negative *(E. coli)* and gram positive *(S. aureus)* bacteria and their biocompatibility on L929 mouse fibroblast cell line,

were targeted.

1.3 Hypothesis

It is stated in many studies that diseases caused by antibiotic-resistant bacteria will increase with a high acceleration and the effectiveness of existing antibiotics against these bacteria will be limited. For this reason, it is important to develop new materials with different action mechanisms than antibiotics.

At this point, inherently antibacterial and biocompatible cationic polymers, which have the advantage of not causing multi-drug resistance, are good examples of such alternatives. As an example of such polymers is P4VP, a polycation with pyridine rings that can be quaternized to obtain pH-independent positively charged groups.

In this study, polymeric nanoparticle-integrated antibacterial cryogel was produced using 4VP and OEGMA monomers. While macroporous cationic 4VP-OEGMA cryogel ensures the absorption of bacterial culture and damaging their membrane, we hypothesized that the 4VP-based cationic nanoparticles on the cryogel surface will increase the antibacterial activity due to the increase in its surface area.

It is suggested that the produced material has the potential to be used in the production of surfaces with high antibacterial activity, porous systems, and bacterial sensor systems.

2
THEORETICAL INFORMATION

2.1 Hydrogels, Cryogels and Cryogelation

Hydrogels are swollen polymeric networks in which hydrophilic polymer chains are cross-linked with each other through physical or chemical bonds [25]. Hydrogels have the ability to detain enormous amounts of water while keeping their structure stable. Due to these properties, in addition to their potential to mimic the biological environment, hydrogels have found extensive application in the fields of drug delivery, tissue engineering, and regenerative medicine. The choice of polymers for using hydrogels in biomedical applications is limited since they must be biocompatible, non-toxic and non-immunogenic, sterilizable, and ensure the in-vivo stability or biodegradation rates depending on the needs [26]. In the applications of tissue engineering and regenerative medicine, to facilitate cell migration, proliferation, and metabolic activity as well as to offer enough mechanical strength and stability in the body, the hydrogel structure should typically be porous with a high degree of pore interconnectivity, as well as they should mimic the extracellular matrix (ECM) in order to help in cell adhesion and proliferation [26].

2.1.1 Classification on Hydrogels

Hydrogels can be classified with respect to their origin, properties, structure, pore sizes, or the type of cross-linking [27]. Some of these classifications are illustrated in Figure 2.1.

- According to their origin, hydrogels can be natural, which are generally synthesized from polysaccharides like chitosan, cellulose, and hyaluronic acid, or polypeptide chains, such as collagen or polynucleotides; synthetic, which are made of synthetic polymers like poly(ethylene glycol) and poly(acrylamide); or hybrid in which it is made up of a combination of both natural and synthetic polymers [27], [28].

- The classification criteria may also include the kind of cross-linking agents; physical, chemical, or biological hydrogels are all viable. The physical hydrogels can be formed when environmental factors, such as temperature, ionic concentration, pH, or other parameters change, turning the polymer solution from a liquid to a gel. In contrast to these weak materials, chemical hydrogels use covalent bonding to add mechanical integrity and degradation resistance to the structure of the gel. In biochemical hydrogels, the gelation reaction is aided by biological components like enzymes or amino acids [27].
- The ionic charges on the bonded groups determine whether a hydrogel is non-ionic, cationic, anionic, or zwitterionic [28].
- According to their pore size, hydrogels can be macro-, micro-, or nano- (or meso-) porous.
- Hydrogels can also be categorized depending to the way they are structured to be amorphous, semicrystalline, crystalline, or hydrocolloid aggregates [29].

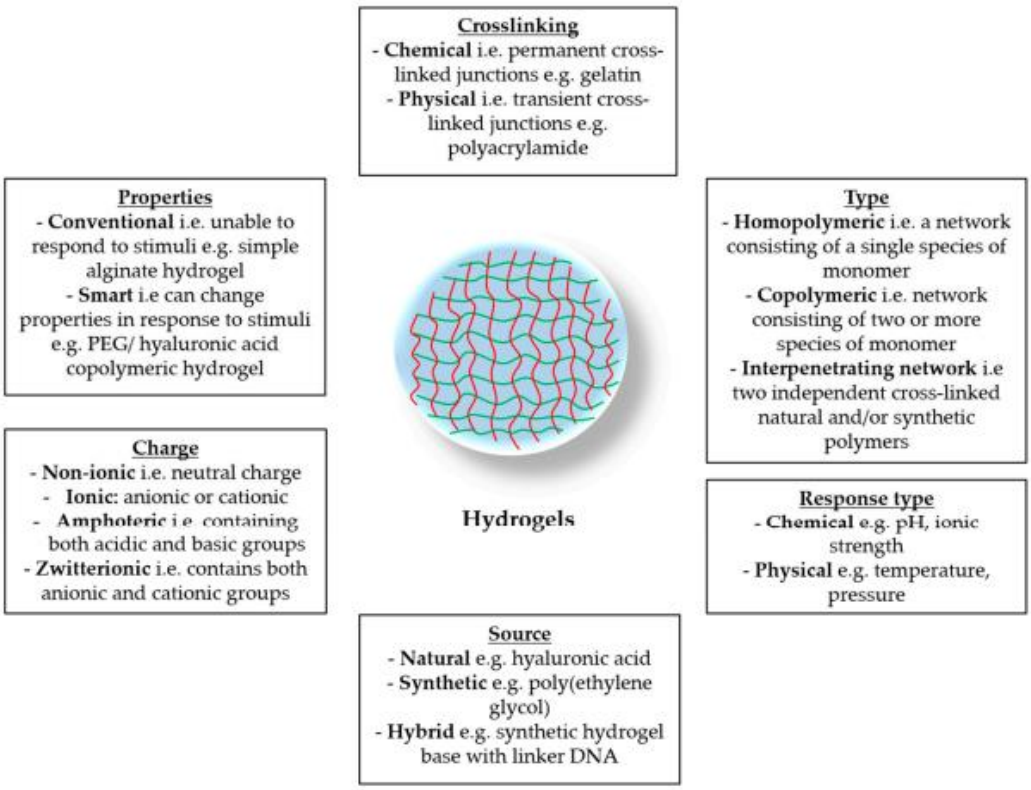

Figure 2.1 The classification of hydrogels [28]

2.1.2 Porosity of Hydrogels

Conventional hydrogels generally have nano-sized pores, and as a result, they have some limitations that make them unsuitable for some biomedical applications such tissue engineering and regenerative medicine due to their physical structure [30]. These limitations include a constrained supply of oxygen and nutrients, issues in seeding cells and challenging integration between the nano-porous hydrogel and the regenerated tissue. To overcome these drawbacks of nano-porous hydrogels in such applications, new methods for preparing macroporous hydrogels have been developed to generate appropriate pore sized hydrogels to avoid the restriction of pore size on the cell behavior [30], [31].

Several methods are used to synthesize and control the porous structure of hydrogels summarized in Figure 2.2. These methods include gas foaming, freeze-drying, phase separation, electrospinning, 3D printing and solvent casting etc. [31], [32]. It is possible to develop porous hydrogels with the desired pore shape and size thanks to the techniques for synthesizing these 3D networks [33].

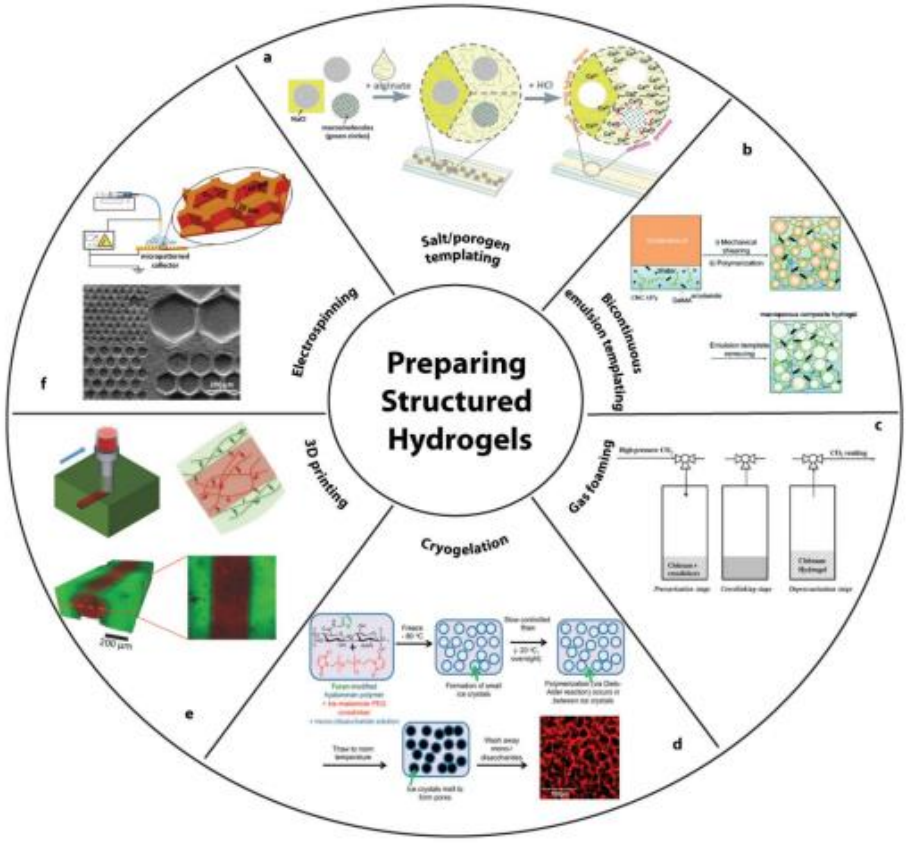

Figure 2.2 Some of the preparation methods of hydrogels [31]

The porosity can be efficiently managed in processes like the leaching of solid particles by adjusting the quantity and size of the pore former (porogen). The variable porosity in the phase separation process is caused by temperature fluctuations and the concentration of the polymer solution. Furthermore, the concentration and viscosity of the polymer solution, as well as the amount of dispersed aqueous phase in the emulsion, determine the porosity in methods, such as emulsion freeze-drying. Unlike gas foaming, which needs organic solvents, the melt molding approach allows for the production of scaffolds in a wide range of shapes and sizes. Each of these traditional methods, nevertheless, has a number of drawbacks [33], [34]. Currently, the main aim is to enhance conventional methods or combine them with other ways to overcome their drawbacks and limitations.

A flexible, effective, economical, and practical method for creating macroporous biomaterials is cryotropic gelation [30], [35], [36]. The cryotropic gelation approach has been proven to be advantageous when compared to other traditional techniques which rely on physicochemical disruptions in the hydrogel solution produced by utilizing porogens [35].

2.1.3 Cryotropic Gelation

The use of cryotropic gelation (cryogelation) as a technique for creating 3D porous hydrogels has received a lot of attention in the last decades [37], [38]. The cryotropic gelation occurs using solvent freezing to form pores in hydrogel material [39]. Following cryotropic gelation, a stable inherently interconnected macroporous hydrogel so called cryogel is formed after the thawing process [14] (Figure 2.3). When a sample is kept under freezing temperatures at -12°C to -20°C, physical or chemical cross-linking takes place in the sample, leading to the formation of a cryogel [34], [38]. As seen in Figure 2.2, this method involves the mixing of monomers and/or polymers in an aqueous solvent, followed by an incubation at extremely low temperatures to promote cryopolymerization and/or gelation as well as the generation of ice crystals, which serve as a porogen during the polymerization process. At the end of the reaction, and when the obtained gels are washed at room temperature to remove unreacted monomers or polymers, the

ice crystals melt and leave behind large interconnecting macro-pores within the cryogel [40].

When compared to other conventional techniques that rely on physicochemical interruptions in the hydrogel solution generated by adding porogens, such as silica, sugar, salt and others, that should be eliminated after the gelation reaction, cryotropic gelation method has been found to be favorable [35]. To avoid damaging cells, these pore-forming units must be carefully removed, but this is a challenging task that could lead to chemical contamination of the material as well as insufficient pore connectivity [36]. On the other hand, cryotropic gelation has proven to be a flexible, efficient, and useful technique for producing porous materials [35], [36], [41].

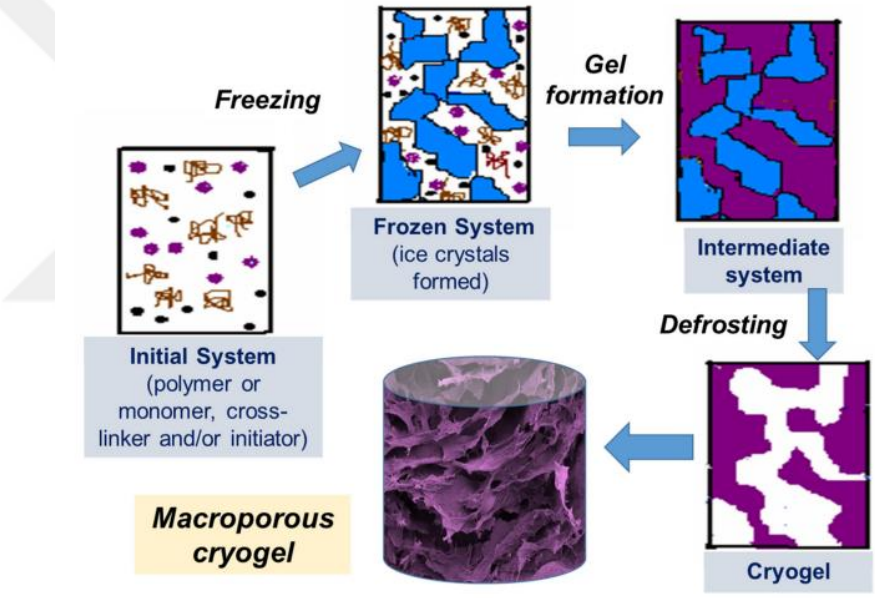

Figure 2.3 The steps of producing macroporous cryogel with cryogelation method [26]

The most common method for cryogelation is synthesizing cryogels via free-radical polymerization. In this reaction, vinyl monomers are often used as gel-forming components along with ammonium persulfate (APS) and tetramethyl ethylenediamine (TEMED) as initiator/catalyst system. The cryogel characteristics can be adjusted for a particular application by adjusting the cryotropic gelation parameters, such as the cooling rate, freezing temperature, presence of ions or other solutes, as well as the amount of polymer and solvent [26]. Other methods

include self-assembling supramolecular gelators, irradiating the polymer solution or suspensions with gamma rays (electron beam, UV), or modified polymers.

2.1.4 Properties and Application Areas of Cryogels

Due to their macroporous structure, which enable efficient mass transport of macromolecular substances, their accessibility for cellular seeding and migration, adaptable mechanical performance, high micro-environmental biocompatibility, and highly hydrophilic interior systems equivalent to the native state of bulk liquid, cryogels have a larger variety of potential applications than conventional hydrogels [42]. By adjusting the concentration of both polymers and cross-linkers, temperature, cooling rate and freezing time, cryogels' mechanical properties can be customized to meet the needs of various applications [43]. A more rapid swelling kinetic and enhanced viscoelastic characteristics that prevent physical deformation are both achieved by the sponge-like macroporous architecture of cryogels. Moreover, unlike the constrained diffusion capabilities present in conventional homophase nano-porous hydrogels, macroporous cryogels enable the unlimited mass transport of solutes, including the facilitation of cellular infiltration and trafficking [41], [44].

Cryogels are ideal bio-scaffold platforms for tissue engineering due to their features, particularly their macroporous structure. Additionally, the dimension of the macropores seen in cryogels can range from a few micrometers to hundreds of micrometers [45]. Cryogels possess a technological advantage over hydrogels because of these key advantages. As a result, developing new cryogels is currently showing to be an important and efficient alternative to conventional bioengineering techniques for tissue regeneration [35], [46]. The potential of cryogels for bioreactors, cell separation, chromatography, and scaffolding has been demonstrated by recent research, proving that they are unquestionably an advantageous matrix for usage in a growing number of applications (Figure 2.4) [15]. Moreover, cryogels can be a promising option when designing antibacterial materials due to their macroporous structure, which facilitate its use within biological molecules without issues with diffusion, in addition to their extremely high mechanical strength and super-fast swelling.

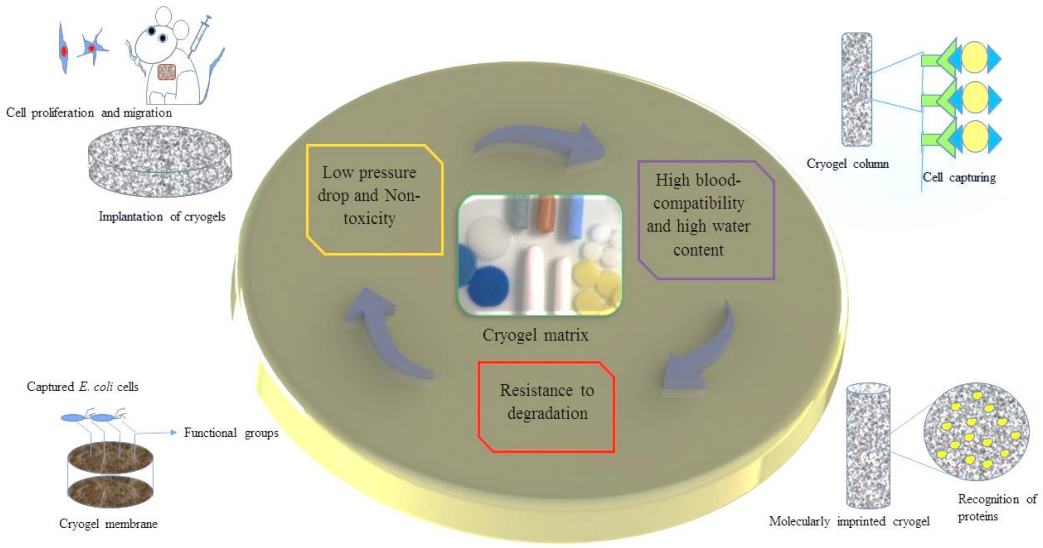

Figure 2.4 Properties and applications of cryogels [10]

2.2 Antibacterial Cryogels

One of the biggest problems threatening the health system worldwide is pathogenic bacterial multidrug resistance to antibiotics. In recent years, the dramatic increase in the mortality rate due to bacterial infections poses a great threat to public health [47]–[49]. In order to control the use of antibiotics while simultaneously having an antibacterial effect, the search for alternative materials as well as the development of new production methods have become crucial goals due to antibiotics' limitations as a treatment against bacterial infections [50], [51]. Due to their macroporous structure that makes them able to be used while working with biological molecules without diffusion issues, in addition to their high mechanical strength and super-fast swelling, cryogels can be considered as a good choice in designing such biomaterials [10], [13]. Antibacterial cryogels can be both antibacterial agent-integrated [52], [53] or inherently antibacterial made up of antibacterial polycations or peptides [54].

2.2.1 Inherently Antibacterial Cryogels

Inherently antibacterial cryogels may also be a viable alternative to conventional antibiotic treatments [11]. It is predicted that the use of antibacterial macroporous cryogels may also have an important application in the treatment of antibiotic resistant pathogens. Therefore, efforts are being made to design and synthesize antibacterial cryogels from inherently antibacterial polymers.

Antibacterial polymers are materials that have been frequently studied in recent years because of their ease of production, cost advantages, high efficiency, and effectiveness [55]. In the production of antibacterial polymeric biomaterials, polycations, which are polyelectrolytes carrying positive charges in their structures, have come to the fore due to their inherently antibacterial activity potential [4]. These polymers break the cell membrane and cause cell bursting by electrostatically cooperative interactions of their positively charged groups with the negatively charged cell membrane components of bacteria as a result of the entry of the polycation into the phospholipid membrane bilayer as illustrated in Figure 2.5 [5].

It is also known that the hydrophobic groups present in their structure or added to it later, make polycations able to destroy the bacterial cell membranes and cause the death of the cells [5]. Polymers, such as chitosan, quaternized poly(4-vinylpyridine) (QP4VP), polyethyleneimine (PEI), and polylysine are among the best-known examples of polycations.

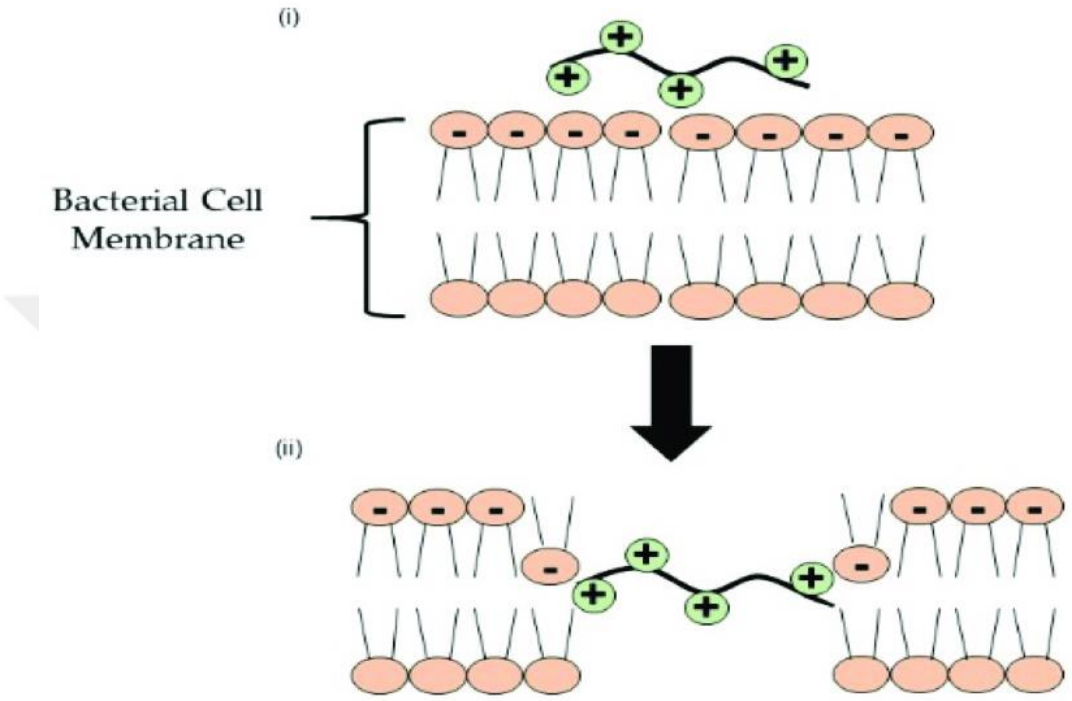

Figure 2.5 The antibacterial mechanism of polycations [7]

A naturally occurring cationic polysaccharide with biocompatibility, antimicrobial activity, and efficient hemostatic performance is chitosan [56]. Due to their ability to form cationic clusters under acidic conditions, chitosan-based hemostatic medicines including Chitoflex, Celox-A, and ChitoGauze have previously received FDA approval and can connect with negatively charged blood cells and proteins to promote coagulation and antibacterial activity [16]. However, because chitosan is poorly soluble at pH levels above 6.5, its antibacterial effect is constrained. For that reason, chitosan is usually combined with other components that increase its solubility at basic pH levels, such as glycidyl trimethylammonium chloride (GTMAC) [16], [57], [58] and polydopamine (PDA) [59].

Antibacterial polymers containing both quaternized ammonium groups and hydrophobic groups, such as QP4VP (Figure 2.6), can be obtained by the

quaternization of pyridine groups with alkyl or benzyl halides [5]. QP4VP has been used as quaternized homopolymer and copolymers in antibacterial material studies and has been found to be effective on various microorganisms, including bacteria, virus, and fungal cells [60]. However, a major disadvantage of the use of quaternary ammonium group-containing polycations, such as QP4VP is that their use in biomaterials becomes limited due to their low biocompatibility [5]. For this reason, the use of QP4VP for antibacterial purposes by making it biocompatible is an important research topic. In recent years, it has been tried to reduce the damage to mammalian cells to very low levels by forming copolymers with hydrophilic monomers, such as poly(ethylene glycol) methylether methacrylate (PEGMA) or 2-hydroxyethyl methacrylate (HEMA), which increase the biocompatibility of these polycations [55], [60].

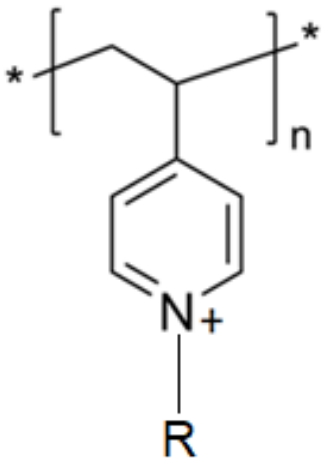

Figure 2.6 Quaternized poly(4-vinylpyridine)

Polyethyleneimine (PEI) is a polycation that has antibacterial activity but its use as a biomedical material is very limited due to its cytotoxicity [61]. Hence, PEI derivatives can be combined with other biocompatible polymers rather than PEI alone to improve its biocompatibility [62].

Because of the presence of both cationic and hydrophobic amino acid residues, cationic peptides have an amphiphilic structure [8]. This characteristic enhances the electrostatic interactions that result from the interaction of positively charged antibacterial peptides and negative-charged bacterial membranes [8]. A cationic polypeptide ε-polylysine was investigated as a potential antibacterial agent [63].

So, cationic polypeptides, such as polylysine and its derivatives can also be utilized on its own to make cryogels that are inherently antibacterial.

2.2.2 Antibacterial Agent-Integrated Cryogels

Cryogels can also be further functionalized with antibacterial agents for related applications. The integration of antibacterial agents, for example, into wound dressings is a critical requirement for non-healing wound care since bacterial infection of the wound is a potentially fatal state, as bacteria tend to cluster under the wound dressing forming a defense layer known as biofilm [64]. In biomedical applications, it is important to highlight that both the antibacterial agent and its by-products must be biocompatible. Cryogels to be used as antibacterial materials can be functionalized with a variety of antibacterial agents including antibiotics and antibacterial nanoparticles especially, metallic nanoparticles.

Antibiotics are unquestionably the most widespread and efficient antibacterial agents, despite having been developed after metal antibacterial agents [48], [65]. The primary issue in the production and administration of antibiotics, however, has been bacteria's ability to build drug resistance. Instead of developing novel antibiotics, it is more advantageous to decrease the doses of currently available antibiotics. Recent years have seen an increased interest in local antibiotic administration [65], which involves administering the proper dosage of the antibiotics directly to the infected area without significantly exceeding the systemic toxicity level. Cryogels can be an excellent choice as local administration matrix, as they provide a high surface area to volume ratio as well as controllable porosity, to mimic biological tissues [66]. Antibiotic-loaded cryogels can selectively release the antibiotics they have been loaded with to the targeted area while preserving high water contents and high biocompatibility. Poly(vinyl alcohol) PVA [67], chitosan [67], starch [68] and gelatin [69] cryogels loaded with antibiotics, such as ciprofloxacin, are some examples of such biomaterials showing antibacterial activity against both gram negative and gram positive bacteria. In addition, ciprofloxacin-loaded PVA/starch cryogels have shown pH, temperature, and composition-sensitive drug release [68]. Moreover, PVA/chitosan cryogel loaded with ciprofloxacin also exhibited pH-sensitive

release [67]. In spite of their drawbacks, antibiotic-loaded cryogels are considered to be better alternatives than uncontrolled administered antibiotics.

Despite the presence of several antibiotic-integrated cryogels in literature, the use of antibiotics is not recommended as antibiotic resistance is growing rapidly, as mentioned above. Furthermore, researchers are still working to find antibacterial agents that are alternatives to antibiotics. Inherently antibacterial nanoparticles can be employed in place of antibiotics because of their nano-scaled size and extremely high surface area to volume ratio, which increase their bioavailability [70]. Over the past few years, an increasing number of studies have been undertaking fundamental research on the use of nanotechnology in such applications [23].

Metallic nanoparticles including silver [71], gold [72], and copper [70] nanoparticles which have unique characteristics that differentiate them from other nanomaterials and exhibit inherently antibacterial activity, have been developed as a new class of biomaterials.

The most commonly used antibacterial metallic nanoparticles are the silver nanoparticles (Ag NPs), which are used in many applications as antibacterial agents in wound dressings [73], contact lenses coating [74], and burn treatment [75]. In addition, these nanoparticles exhibited antiviral activity against cells that were HIV-infected [76]. However, due to problems with dispersion and dissolution that could reduce their efficiency and have possible (ecological) toxicity, the practical uses of free Ag NPs are still limited. To minimize this problem, Ag NPs can be embedded in cryogels. There are many designed Ag NPs-embedded cryogels in literature. For example, Ag NPs embedded poly(sodium acrylate) cryogels [19], and cationic starch and nano-fibrillated cellulose cryogels [20], showed antibacterial activity against both gram negative and gram positive bacteria. In wound dressing, poly(2-hydroxyethyl methacrylate-glycidyl methacrylate) (poly(HEMA-GMA)) [21], chitosan [22], and gelatin cryogels decorated with Ag NPs have the potential to promote wound healing simultaneously with anti-biofilm activity, antibacterial, and hemostasis potential.

Another commonly used antibacterial metallic nanoparticles are gold nanoparticles (Au NPs). Although these nanoparticles have numerous uses, their significance in various industries could devalue as a result of their aggregation problem. To solve this issue, particular templates have been employed as a solution. Hydrogels and microgels are two of these templates that are frequently used by researchers in order to use such nanoparticles in biomedical applications [78]. Poly(N-isopropylacrylamide) (NIPAM) and sodium 2-acrylamido-2-methyl propyl sulfonate (AMPS-Na) monomers [78] in addition to chitosan [72] based cryogels containing Au NPs have enhanced wound healing in addition to having antibacterial activities.

Inherently antibacterial polymeric nanoparticles are thought to be an ideal alternative to antibiotics and metallic nanoparticles [1], [79], because of their easy production, biocompatibility in addition to the ability to control their size, charge, and biodegradability according to the aim of the study [80]. The number of antibacterial polymeric nanoparticle-integrated cryogels is very limited, antibacterial polymeric micro-, macro-, and nanoparticles prepared from poly(tannic acid) embedded in HEMA-based cryogels was found to have antibacterial activity against gram negative bacteria [24]. It is suggested that antibacterial polymeric nanoparticle-integrated cryogels might be an effective alternative to antibiotic and metallic nanoparticle-integrated cryogels because of their controllable properties in addition to their biocompatibility.

2.2.3 Applications of Antibacterial Cryogels

Their superior mechanical properties, antibacterial activity, large pore size ranging between 10 to 200 μm, biocompatibility, and short diffusion paths make cryogels a promising material to be used in many applications [14], such as tissue engineering [15], wound dressing [16], and water treatment [17].

The ECM plays a critical role in creating the ideal environment for cell interactions and signaling. The discipline of tissue engineering makes it possible to replicate such a matrix in order to facilitate tissue repair and recovery [30], [32]. While there are a variety of techniques to construct scaffolds, cryogels have lately gained popularity due to their strength and macroporous nature [10], [15], [35]. For

instance, cryogels have been the subject of numerous research as a viable bone graft alternative for applications involving bone regeneration, as bone graft used in tissue engineering has a number of drawbacks, such as excessive cost, infection risk, and donor site complication [15]. In addition, cryogels have also been loaded with antibacterial agents, such as antibiotics [81] and silver nanoparticles [82], [83] for the treatment of possible bone infections.

Moreover, antibacterial cryogels are an outstanding choice for wound dressings to minimize infection potential while enhancing wounds healing [12]. As uncontrolled hemorrhage accounts for over 30% of all trauma deaths globally, improving patient survival through emergency medicine care that includes quick interventions with hemostatic agents is important [84]. For that reason, it is important to develop new, multifunctional hemostatic materials that can rapidly and efficiently control excessive bleeding from deep wounds, eliminate bacteria at the wound, and speed the process of healing [16]. Therefore, cryogels synthesized using antibacterial polymers, such as chitosan [16], HPMA [18], QP4VP [85], etc. in addition to cryogels loaded with antibacterial agents have recently come to light as a viable option for lowering infection and enhancing wound healing [12].

2.3 Bacteria and Bacterial Infections

According to their cell type, cellular organisms are divided into prokaryotes and eukaryotes [86] (Figure 2.7). Prokaryotes typically have smaller, and more simple structures. These prokaryotic cells include bacteria, which lack organelles and nuclei. However, bacteria also have components including cytoplasm, ribosomes, and plasma membranes that are present in all other cellular organisms [86].

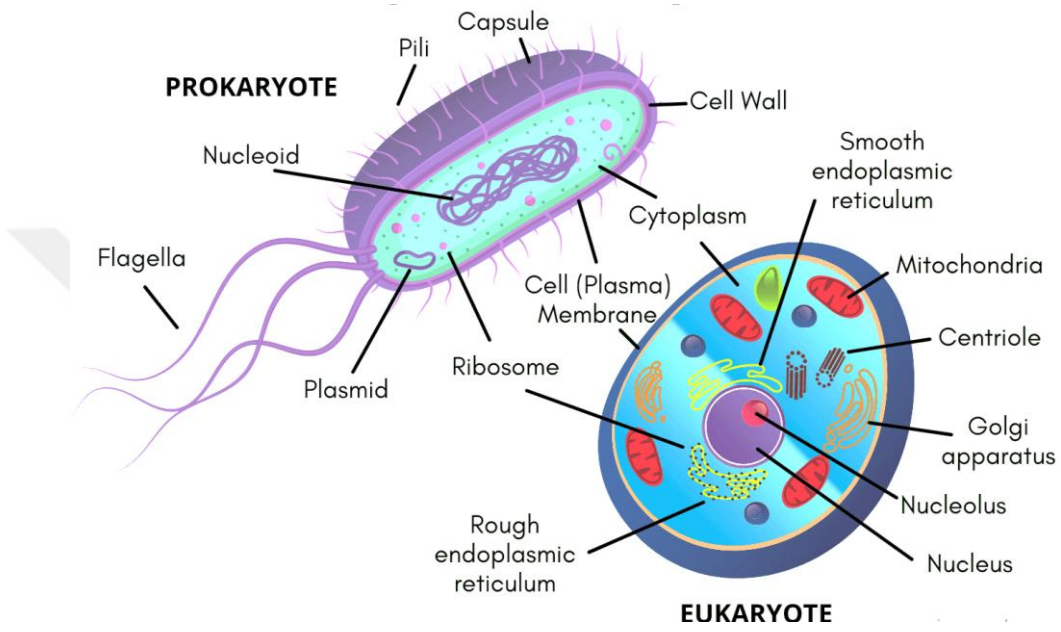

Figure 2.7 The structure of prokaryotic and eukaryotic cells [87]

Bacterial cell wall, which is present in the majority of bacteria, is a layer with a semi-solid structure that gives the cell membrane some rigidity and strength. Gram positive and gram negative bacteria are the two strains of bacteria that are classified with respect to their cell walls' structural differences as shown in Figure 2.8 [88]. Gram positive bacteria have a continuous, relatively thick cell wall mainly made up of peptidoglycans covalently bonded with various cell wall polymers, including teichoic acids, polysaccharides and peptidoglycolipids [89]. On the other hand, the cell wall in gram negative bacteria is double layered, containing a cellular membrane outside the peptidoglycan thin layer. In addition, gram negative bacteria have two regions surrounding the outer plasma membrane: the periplasmic space which is relatively small in gram positive bacteria, if present, and the lipopolysaccharide layer which is absent in gram positive bacteria [86], [88].

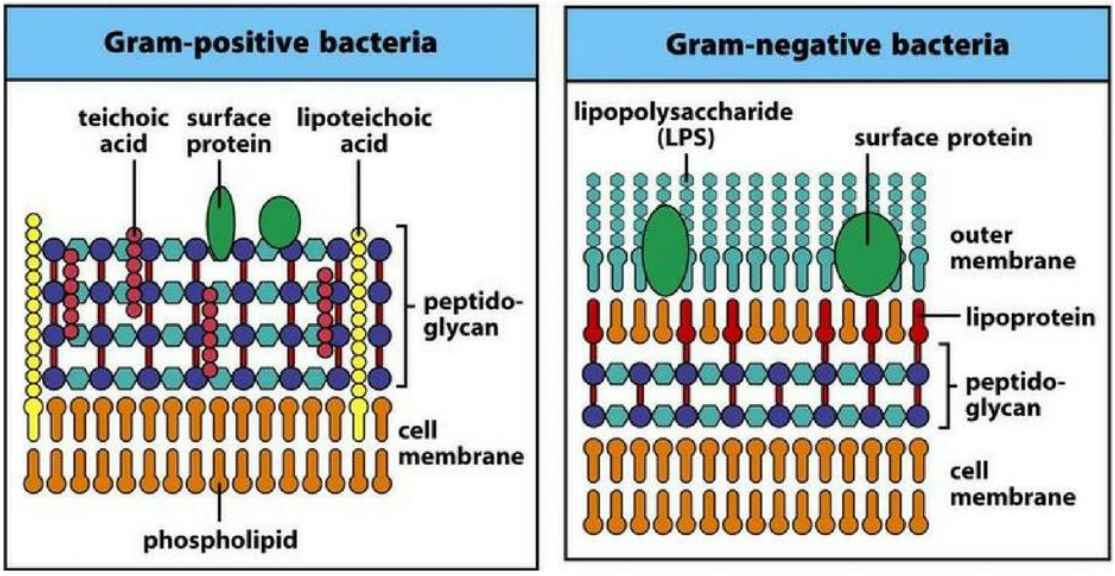

Figure 2.8 The cell wall of gram positive and gram negative bacteria [90]

2.3.1 Bacterial Infections

Even though the vast majority of bacteria are harmless and some even aid in digestion and fighting against opportunistic pathogens, bacterial infections are among the most common conditions that affect human health [91]. Due to the increasing antibiotic resistance, bacterial infection represents a serious threat to human health. It is crucial to identify and treat pathogenic microorganisms early and efficiently, since they can cause excessive morbidity and mortality [6]. The normal cohabitation of bacteria and host cells seen in healthy people is disrupted in bacterial pathogenesis [1]. Most frequently, these infections develop when bacteria move from regions with a normal microbiota, such as the mucosal lining of the nose and mouth, to those with abnormal colonization like lung, blood, kidney, etc. This bacterial translocation may be aided by both long-term implants, including screws, joint implants, and cardiac devices, in addition to temporary implants, such as intubation tube, urinary catheter, etc. that connect between these two physiological regions [1].

The most typical course of treatment for bacterial infections is still antibiotics [48], [65]. These and other antibacterial agents' mechanisms of action can be divided into two main classes, these are membrane and intracellular dysregulations:

- When medicines directly interact with intracellular constituents to destabilize homeostasis, intracellular dysregulation occurs.
- On the other hand, membrane breakdown, loss of nutrients uptake, and/or changes in interior concentration of ions are all consequences of membrane dysregulation, which involves therapeutic interactions that allow changes in membrane rigidity, polarity, and permeability [1].

While antimicrobials like positively charged antimicrobial peptides (AmPs) interact with the negatively charged teichoic acids of the cell membrane to produce gaps [92], antibiotics selectively attach to the penicillin-binding protein inside the cell membranes of many bacteria, inhibiting cell wall production [8]. It is more important than ever that we keep developing efficient techniques for identifying and treating bacterial infections [4], [5], because bacterial resistance to modern antibiotics is on the rise, in which bacteria may find alternative metabolic pathways, produce antibiotic-inactivating enzymes, modify its membrane permeability, or the antibiotic might be eliminated from the bacteria through efflux pumps as illustrated in Figure 2.9 [2].

Antibiotic resistance has been attributed to the excessive usage of antibiotics. Antibiotic resistance is anticipated to increase as a result of the COVID-19 pandemic due to the staggeringly high number of hospitalized patients who are getting antibiotics for treating suspected secondary infections [1], [3]. Promising antimicrobial agents that may cause less of a worry regarding resistance include synthetic and natural polymers, AmPs, and repurposed medications.

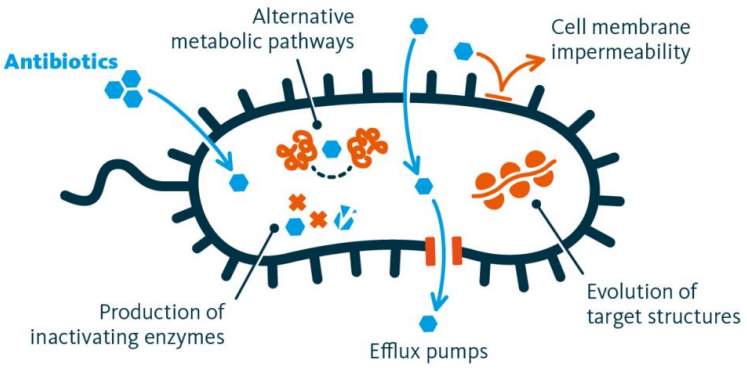

Figure 2.9 The mechanism of antibiotic resistance [93]

There has been significant advancement in the designing of easier, more efficient, and more affordable methods for the detection for monitoring the progress of bacterial infections in recent years. Natural and synthetic polymers, as well as their derivatives, offer enormous antibacterial potential [5]. Recent advancements have concentrated on synthetic antibacterial polypeptides and polymers due to the flexibility of synthetic techniques. These macromolecules are more scalable and cost-effective than AmPs and frequently mimic the physical and chemical characteristics that give them their antibacterial action [7], [8]. Quaternary ammonium polymers, polymethacrylates, poly [2-(dimethyl decyl ammonium) ethyl methacrylate], poly-ß-peptides, and polyimidazolium are a few prevalent examples [5], [6]. Investigations into the relation between the structure of the polymer and the antibacterial activity of various antibacterial agents revealed that main chain polycations exhibit higher antibacterial activity than side chain ones [5].

Additionally, it was also observed that the side chain / main chain polycations, made up from small cationic compounds, such as quaternary ammonium, showed higher antibacterial activity than their corresponding small molecule cationic compounds. These polymers efficiently suppressed the proliferation of the gram negative *E. coli* and the gram positive *S. aureus* particularly [6].

Biomaterials are utilized in antibacterial therapy as inherently antibacterial agents and/or antibacterial-agent carriers [1], [6], [12]. Additionally, by acting as delivery systems for antibacterial agents, biomaterials have the potential to lower the risk of infection, improve treatment efficiency, and decrease the host toxicity. Antibacterial drug delivery systems and surface coatings have gathered a lot of attention in this research area. These biomaterials can range from the nano-scaled polymers [5] and metal nanoparticles [9] to the macro-sized thin films and hydrogels [10]–[12].

In this study, 4VP-based cationic nanoparticle-integrated antibacterial 4VP-OEGMA cryogels were produced and their antibacterial activity and biocompatibility were investigated. It is suggested that produced cryogel has the potential to be used as antibacterial biomaterial in many biomedical applications.

3
MATERIALS AND METHOD

3.1 Materials

Table 3.1 List of chemicals used in the study

Chemical Name	Supplier	Purpose of Usage
1,6-Dibromohexane	Sigma-Aldrich	Cross-linker
1-Bromohexane	Sigma-Aldrich	Alkylating agent
3-(4,5-dimethylthiazol-2yl)-2,5-diphenyltetrazolium bromide (MTT)	Biomatik	Cytotoxicity Test
4,4'-Azobis(4-cyanovaleric acid) (ACVA)	Sigma-Aldrich	Initiator
4′,6-diamidino-2-phenylindole (DAPI)	Serva	Staining
4-Vinylpyridine (4VP)	Sigma-Aldrich	Monomer
Acetone	TEKKİM Kimya	Solvent
Ammonium persulfate (APS)	Sigma-Aldrich	Initiator
Diethyl ether	Sigma-Aldrich	Solvent
Dimethyl sulfoxide (DMSO)	Sigma Aldrich	Cell Culture
Dulbecco's Modified Eagle Medium (DMEM/F12)	Capricorn	Cell Culture
Ethanol	TEKKİM Kimya	Organic solvent / Sterilization
Fetal Bovine Serum (FBS)	Capricorn	Cell Culture
Fibroblast cell line (L929)	YTU / Department of Bioengineering / Cell Culture Laboratory	Cell Culture
Isopropyl alcohol (2-Propanol)	TEKKİM Kimya	Organic solvent

Table 3.1 List of chemicals used in the study (continued)

Methanol	TEKKİM Kimya	DAPI staining
Mueller-Hinton Agar	Merck	Microbial Culture Medium
Mueller-Hinton Broth (MHB)	Merck	Microbial Culture Medium
N,N,N′,N′-Tetramethyl ethylenediamine (TEMED)	Sigma-Aldrich	Catalyst
N,N'-Dimethylformamide (DMF)	ISOLAB	Solvent
N,N'-Methylenebisacrylamide (BAAm)	Sigma-Aldrich	Cross-linker
Penicillin-streptomycin	Capricorn	Cell Culture
Polyethyleneglycol methyl ether methacrylate (OEGMA-500)	Sigma-Aldrich	Monomer
Staphylococcus aureus (S. aureus) (ATCC 25923) and *Escherichia coli (E. coli)* (ATCC 25922) strains	YTU / Department of Molecular Biology and Genetics / Microbiology Laboratory	Microorganism Strains
Trypsin-EDTA (0.25%)	Sigma Aldrich	Cell Culture

3.2 Equipment

Table 3.2 List of equipment used in the study

Name of the Equipment	Brand/Model
Analytical balance	Sartorius CP225D
Biological Safety Cabinet	ESCO Class II
Centrifuge	Himac
Cryostat	KERMANlab
Drying oven	Binder
Dynamic and Electrophoretic Light Scattering Spectroscopy	Malvern Zetasizer Nano-ZS
Fluorescence microscope	Olympus
Freeze dryer	Heto / Drywinner DW 1.0-60e
FTIR	Thermo Scientific / Nicolet iS10 FTIR with ATR attachment
GPC	Viscotek TDA302
Incubator	Binder and Memmert UN55
Invert microscope	Olympus
Laminar flow cabin	Faster
Magnetic Stirrer	Heidolph MR300
Microplate reader	Multiskan™ FC
NMR Spectroscopy	Bruker Ascend 500 MHz
Refrigerated Centrifuge	Nüve
SEM	ZEISS EVO 10
Shaking Incubator	DaiHan ThermoStable™ IS-20
Texture Analyzer	Texture Technologie / TA.XTPlus Connect
Ultra-pure water device	Millipore MilliQ Gradient
UV-Vis Spectrophotometer	Shimadzu UV-1800
Vacuum oven	Binder
Vortex	Heidolph Reax Top

3.3 Experimental Method

In the study, polymeric antibacterial polymeric nanoparticle-integrated antibacterial cryogels were produced. In the first step, random copolymer of poly(4VP-co-OEGMA) was produced with free radical polymerization. Then, the copolymer was used to prepare positively charged nanoparticles by cross-linking with a bifunctional alkylating agent. In the second step, the cryogels of 4VP and OEGMA were prepared by cross-linking with BAAm. In the final step, nanoparticles were cross-linked on the pore gel walls through quaternization reaction to prepare nanoparticle-integrated cryogels. (Figure 3.1) All the cryogels produced were tested against *E. coli* and *S. aureus* for antibacterial activity and on L929 for biocompatibility.

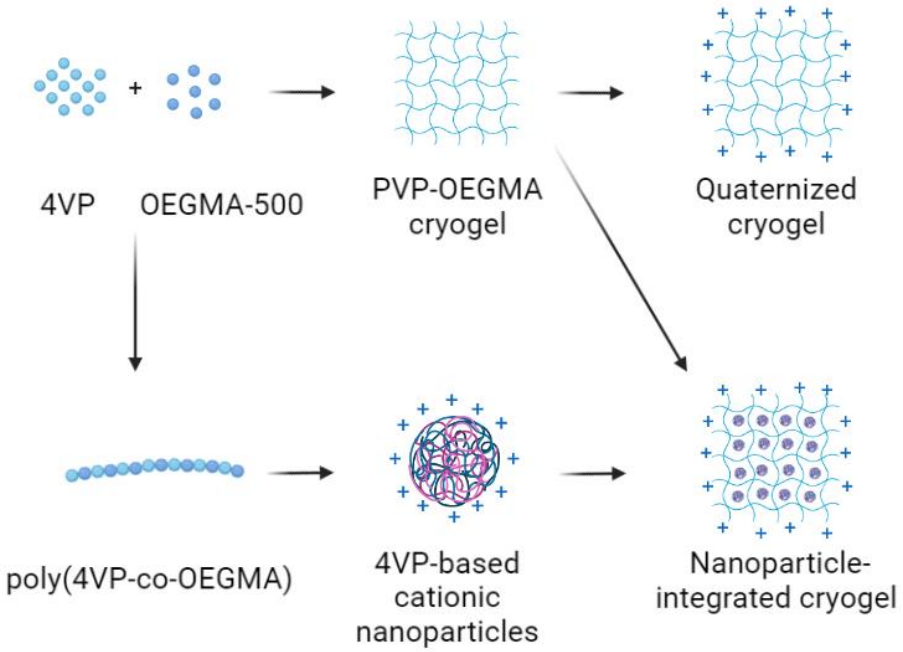

Figure 3.1 Experimental methods of the study

3.3.1 Synthesis of Poly(4VP-co-OEGMA) Random Copolymer

Poly(4VP-co-OEGMA) random copolymer to be used in the synthesis of the nanoparticles, was synthesized using free-radical polymerization method shown in Figure 3.2 [5]. For the reaction, 0.9 M 4VP and 0.1 M OEGMA-500 were dissolved in 10 mL DMF, and the monomer solution was purged with N_2 gas for 15 minutes. Then, the solution was heated to 70°C and the polymerization reaction

started by the addition of the initiator. ACVA was used as the initiator and the molar ratio of monomer:initiator was 100:1. After 24 hours, the obtained copolymer was precipitated with excess cold diethyl ether and washed three times in order to eliminate the unreacted monomers and the remaining DMF. The weight of the produced copolymer was measured to calculate the polymer yield by dividing the weight of the produced polymer to the weight of the added monomers. Finally, the copolymer was dried in a vacuum oven overnight at 50 °C.

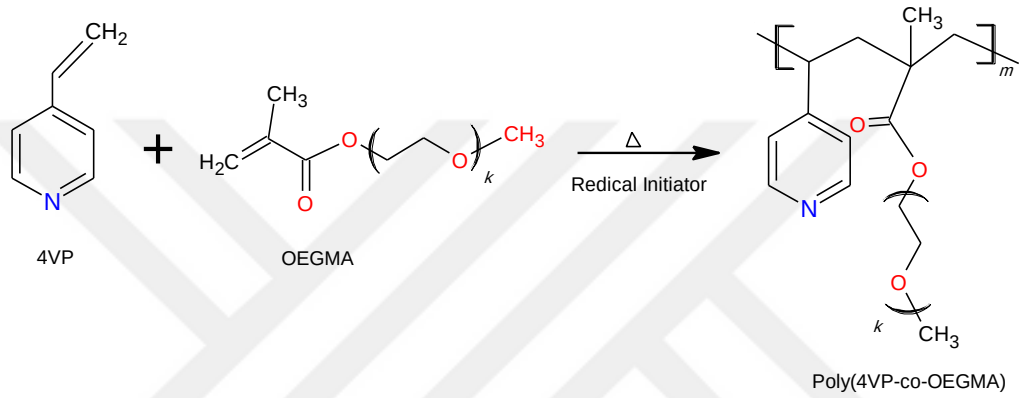

Figure 3.2 The free-radical polymerization reaction of 4VP and OEGMA-500

3.3.2 Synthesis of 4VP-Based Cross-Linked Cationic Nanoparticles

In order to prepare the 4VP-based cross-linked cationic nanoparticles, 6 mg of the synthesized poly(4VP-co-OEGMA) copolymer was dissolved in 2 mL acetone and the cross-linker, 1.2 μL 1,6-dibromohexane, was added to the solution. The solution was added to 20 mL ultra-pure water under vigorous stirring. After the acetone evaporated completely, the quaternization reaction was carried out by heating the aqueous solution at 70°C for 24 hours. The structure of the copolymer after cross-linking is shown in Figure 3.3. At the end of the quaternization reaction, the nanoparticles solution was freeze-dried and characterized. The yield of the produced nanoparticles was calculated by dividing the weight of the produced nanoparticles to the total weight of the initial components added to the reaction.

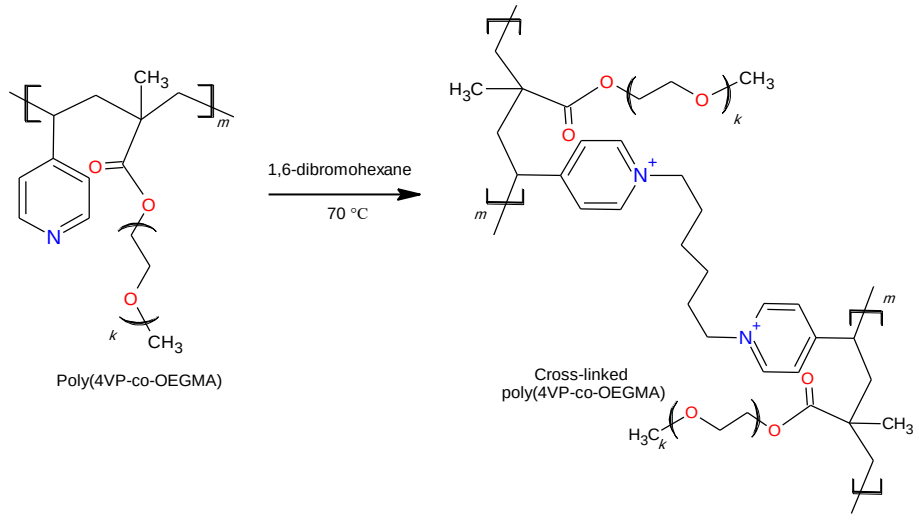

Figure 3.3 Cross-linking of poly(4VP-co-OEGMA) copolymer with quaternization

3.3.3 Synthesis of 4VP-OEGMA Cryogels

For the cryotropic gelation of 4VP and OEGMA using free-radical polymerization, two separate aqueous solutions were prepared. In the first solution, 4VP (69 µL, 0.64 mmol), OEGMA-500 (80 mg, 0.16 mmol), BAAm (12 mg, 0.08 mmol) and TEMED (7.14 µL) were dissolved in ultra-pure water. In this solution, 4VP and OEGMA-500 are the monomers and molar ratio of 4VP:OEGAM was 8:2. BAAM was used as the cross-linker and TEMED was the catalyst for free radical initiator. The second solution was the initiator solution, in which APS (3 mg, 0.013 mmol) was dissolved in ultra-pure water. The molar ratio of monomer:initiator was 100:1.66. N_2 gas was passed through both solutions each for 15 minutes, and after cooling the solutions to +4 °C, APS solution was added to the monomers solution and mixed on vortex. Immediately after mixing, the solution (1 mL) was filled into the syringe and left in the cryostat for 24 hours at -15 °C until the cryogel was formed. The produced cryogels were cut into 1 cm pieces and washed with 2-propanol in order to eliminate any unreacted monomers. Figure 3.4 shows the chemical structure of the obtained 4VP-OEGMA cryogels.

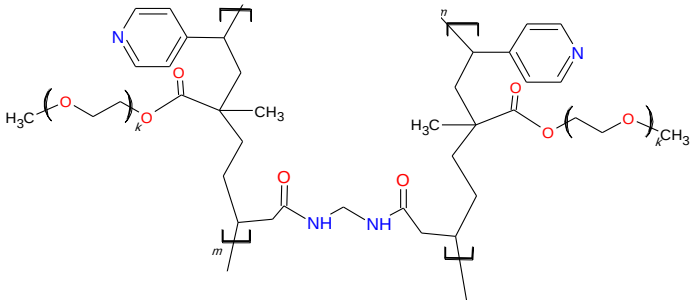

Figure 3.4 The chemical structure of 4VP-OEGMA cryogels

3.3.4 Preparation of Nanoparticle-Integrated 4VP-OEGMA Cryogels

The previously prepared nanoparticles (5 mg) were dissolved in 1 mL 2-propanol solution containing 1,6-dibromohexane (45 µL, 0.3 mmol) and 1-bromohexane (14 µL, 0.1 mmol). Then, a non-quaternized freeze-dried cryogel piece (~20 mg) was immersed into the nanoparticle solution and incubated at 70°C for 4 days. Afterwards, the produced nanoparticle-integrated cryogel was washed with 2-propanol to eliminate the unreacted compounds. Figure 3.5 shows the chemical structure of the synthesized nanoparticle-integrated cryogels.

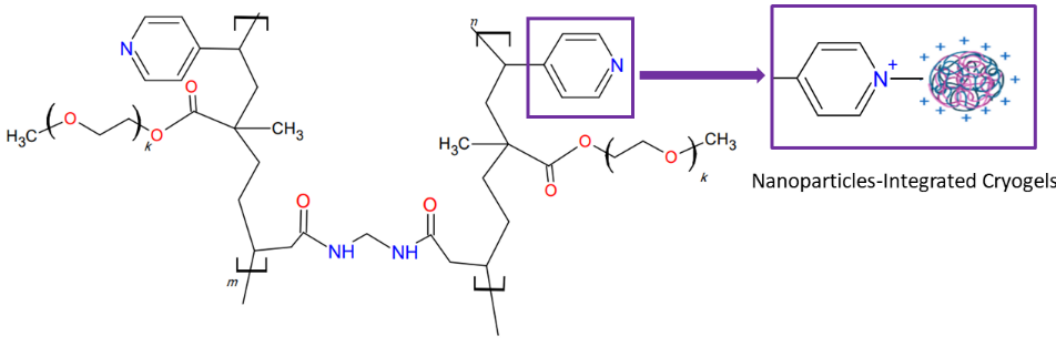

Figure 3.5 The chemical structure of the nanoparticle-integrated cryogels

3.3.5 Quaternization of the Synthesized 4VP-OEGMA Cryogels

4VP groups of previously synthesized cryogels were quaternized with 1-bromohexane. In this reaction, 1-bromohexane (56 µL, 0.4 mmol) was dissolved

in 1mL 2-propanol. The freeze-dried cryogel (~20 mg) was immersed into this solution and incubated at 70°C for 4 days. The chemical structure of the quaternized cryogels is shown in Figure 3.6. The produced quaternized cryogel was washed with 2-propanol to eliminate the unreacted compounds. The quaternization degree of the cryogels was adjusted to be the same as that of the nanoparticle-integrated cryogels.

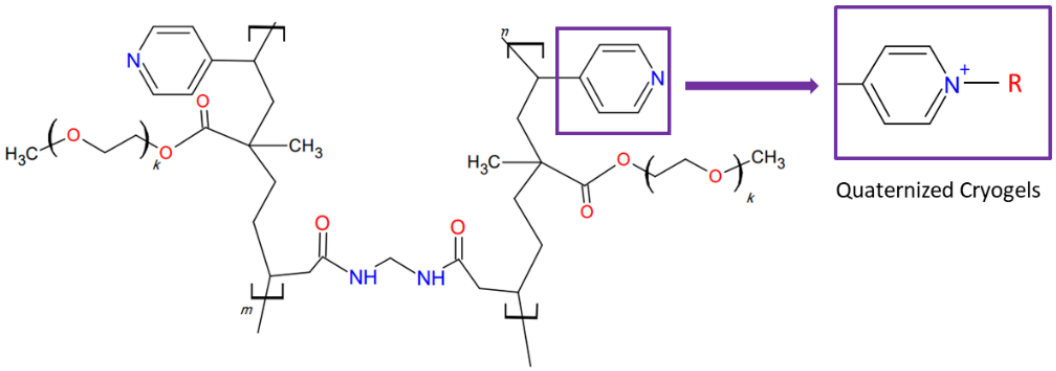

Figure 3.6 The chemical structure of the quaternized cryogels

3.4 Characterizations

3.4.1 Chemical Characterization

- Nuclear Magnetic Resonance (NMR) Spectroscopy

The chemical composition of the synthesized copolymer was examined with Bruker Ascend 500 MHz nuclear magnetic resonance spectroscopy. Polymer was dissolved and prepared in deuterated dimethyl sulfoxide (DMSO) for the analysis. ^{1}H-NMR spectrum of the copolymer was acquired from the analysis.

- Gel Permeation Chromatography (GPC)

The average molecular weights and molecular weight distribution of the synthesized copolymer were found with GPC. CatSEC300 column was used for the analysis performed on Viscotek TDA302 GPC device. As mobile phase, 0.1 M acetic acid (CH_2COOH) and 0.15 M sodium chloride (NaCl) solution was prepared. The polymer sample was prepared at a concentration of 2 mg/mL. The mobile phase and the polymer solution were filtered with 0.45µm filters and degassed in an

ultrasonic water bath before the analysis. Polyethylene oxide (PEO) (M_W = 18.7 kDa, M_W/M_n = 1.05) was used as the calibration standard of GPC. Flow rate was 0.4 mL/min throughout the analysis.

- Fourier-Transform Infrared (FTIR) Spectroscopy

FTIR spectra of the prepared poly(4VP-co-OEGMA) random copolymer, nanoparticles and cryogels were acquired from Shimadzu IRPrestige-21 FTIR with attenuated total reflectance (ATR) attachment at wavenumber range between 4000 and 650 cm^{-1}. All the samples were dried before analysis. FTIR spectra was used for chemical analysis of the materials and determination of the quaternization degrees of nanoparticles and cryogels. The quaternization degrees of the synthesized cryogels were calculated using equation (3.1) [94].

$$Q\% = \frac{A_{1640}}{A_{1640}+(1.68\times A_{1600})} \times 100 \qquad (3.1)$$

Where,

Q% is the quaternization degree, and

A_{1640} and A_{1600} are the absorbance values of the material at the wavenumbers of 1640 and 1600, respectively.

3.4.2 Physical Characterization

- Dynamic and Electrophoretic Light Scattering

The hydrodynamic size and zeta potential value of the synthesized cationic nanoparticles were determined by dynamic and electrophoretic light scattering methods (DLS and ELS, respectively), where the measurements were done by dissolving the freeze-dried nanoparticles in ultra-pure water at room temperature with concentrations of 1 mg/mL for each solution, using Malvern Zetasizer Nano-ZS device equipped with 4.0 mV He-Ne laser at 633 nm at scattering angle with 173º.

- Morphology

The internal morphology of the non-quaternized, quaternized, and nanoparticle-integrated cryogels were examined with scanning electron microscope, in which freeze-dried cryogel samples were coated with gold/palladium composite to

ensure the sample's conductivity, and the images were taken by ZEISS EVO 10 SEM device at 500X and 20,000X magnifications.

- Swelling Studies

The synthesized non-quaternized, quaternized, and nanoparticle-integrated cryogels were cut into approximately 1 cm long pieces and washed with 2-propanol, then with ultra-pure water many times.

To calculate the weight and volume fractions (q_w and q_v, respectively) of the synthesized cryogels, freeze-dried cryogel pieces were swelled in ultra-pure water to determine their masses and volumes ($m_{swollen}$ and $D_{swollen}$) at swelling equilibrium state. After drying the swollen cryogels, masses and volumes (m_{dry} and D_{dry}) at dry state were measured and swelling fractions by weight and volume were calculated using equation (3.2) and (3.3), respectively [95].

$$q_w = \frac{m_{swollen}}{m_{dry}} \quad (3.2)$$

$$q_V = \left(\frac{D_{swollen}}{D_{dry}}\right)^3 \quad (3.3)$$

For swelling kinetics determination, the freeze-dried cryogels were swollen in ultra-pure water and their weight fractions over time were calculated until they reached their swelling equilibrium weight. The obtained results were plotted, and the swelling kinetics behavior of the cryogels was investigated.

3.5 Investigation of the Antibacterial Activity of the Synthesized Cryogels

Preparation of Bacterial Suspensions: *E. coli* and *S. aureus* were grown in MHB at 37 °C for 18 hours. The to be used in the study cultures were diluted with the same broth at an absorbance value of 0.2 ± 0.02 at 600 nm (1.5-3.0 × 10^8 CFU/mL of the microorganism).

Antibacterial Activity Studies: The antibacterial activity of the synthesized non-quaternized, quaternized, and nanoparticle-integrated cryogels was investigated on *S. aureus* and *E. coli* prepared as previously described, but with minor modifications [13]. Briefly, 10 μL of bacterial suspensions were dropped onto the

surface of the gels that were sterilized under UV and then the cryogels containing bacteria were incubated for 30 minutes at room temperature. After that, the samples were replaced into tubes containing 10 ml MHB and incubated for 4 hours at 37 °C. After incubation, the serial dilutions of samples taken from the tubes were spread to MHB-agar, and incubated overnight at 37°C. The following day colony-forming units (CFU) were counted to calculate surviving bacteria. In the study, "only bacteria inoculum" was used as a control tube. The antibacterial activity was evaluated through the logarithmic reduction and the percentage of killing activity on the bacteria using equations (3.4) and (3.5), respectively [96].

$$Log_{10}\, reduction = \ Log_{10}(B) - Log_{10}(A) \qquad (3.4)$$

$$Recution\%\ (CFU/mL) = \frac{B-A}{B} \times 100 \qquad (3.5)$$

where,

A is the CFU per milliliter for the vial containing bacteria treated sample after the specified contact time, and

B is the CFU per milliliter for the 'only bacteria inoculum' vial after the specified contact time

After the samples were incubated for 4 hours at 37 °C for the investigation of their antibacterial activity, a small piece of nanoparticle-integrated cryogel cotaining *S. aureus* was cut and dried to be anlayzed with SEM, in order to ensure the presence of damaged bacteria on their surface.

3.6 Biocompatibility Tests

Cell Culture: Cell culture studies were performed using L929 fibroblast cells [97]. Fibroblast cells in DMEM F/12 growth medium, containing 1% penicillin-streptomycin and 10% FBS, were cultured in an incubator set at 95% humidity, 5% CO_2 and 37°C. Cells were passaged after reaching 70-80% cell density on the flask surface. In the passaging process, the cells were first washed with PBS one time, then cells were collected enzymatically from the surface using 0.25% trypsin-EDTA and centrifuged at 1000 rpm for 5 minutes after adding growth medium. After centrifugation, the supernatant was discarded, and the cell pellet was suspended with 1 mL of growth medium. Cell counts were performed on a

thoma slide using trypan blue. The number of cells required for cell studies was suspended with growth medium and used in the analysis.

Sterilization of Cryogels: Cryogels were cut into 5 mm*2 mm size for sterilization and kept in 75% ethanol for 3 hours. The cryogels were then dried under a fume hood and treated with UV for 30 minutes. Sterile cryogels were incubated in cell growth medium for 3 hours before being treated with cells [98].

Cell viability analysis: The cytotoxicity of the cryogels were analyzed on L929 cells using the direct method [99]. For this analysis, firstly, 25,000 cells were seeded in each well of the 48-well plate and the plate was left to incubate for 24 hours. At the end of this period, sterile cryogels were transferred to the wells and the medium in the wells was adjusted so that it did not overlap the cryogels and had a cell-cryogel interface. The medium of the wells without cryogel was replaced with fresh medium and considered as the control group. After cryogel application, the plates were incubated for 24 hours. The cryogels in the wells were then removed for MTT analysis and the medium aspirated. The cell medium in the wells was washed with PBS and the cells were harvested from the well surface with 0.25% trypsin-EDTA treatment. An equal volume of medium was added for the inhibition of the enzyme in the medium in which the cells were present, and the cells were precipitated in a centrifuge set at 1000 rpm, 5 minutes and 25 ºC. After this procedure, the supernatants were discarded, and the cell pellets were resuspended with an equal amount of medium.

For cell viability analysis, cells belonging to each experimental group were seeded in 96-well plates in triplicate. The plate was incubated for two hours to allow the cells to adhere, and then 10 μL of MTT solution prepared with PBS at a concentration of 10 mg/mL was added to each well and it was left to incubate for 4 hours. During this time, the yellow tetrazolium in the MTT solution is transformed into purple formazan by living cells. In order to dissolve the formazan formed in the wells, 100 μL of DMSO was added to each well and incubated in the darkness for 30 minutes. The optical density in the wells was then measured in a microplate reader to 570 nm.

Cell viability (%) was calculated using the obtained absorbance data using equation (3.6). Three replications were performed for each group and ±SD was calculated.

$$\text{Cell viability (\%)} = (OD_{sample}) / (OD_{control}) \times 100\% \qquad (3.6)$$

DAPI Staining: In order to examine the effect of cryogels on cell density and adhesion, after the cells were treated with cryogels, DAPI nuclei staining was performed and the cells were viewed under a fluorescence microscope [100]. For staining, DAPI dye solution was prepared with PBS at a concentration of 1 μg/mL and kept at +4 ºC. In addition to the plates prepared for cell-cryogel treatment for cell viability analysis, cells were seeded simultaneously for DAPI staining. Wells without cryogel were considered as the control group. 24 hours after cryogel treatment, cryogels and growth medium were removed from the wells and cells were washed with PBS. After this procedure, the cells were fixed in the darkness for 5 minutes with cold methanol, previously stored at -20 ºC. After fixation, methanol was aspirated from the wells and the medium was washed twice with PBS. Then, 500 μL of DAPI dye solution was added to the wells and the plates were incubated in the darkness for 20 minutes, then the dye solution was aspirated. The medium was washed twice with PBS to remove residual dye. Then, the adhesion and density of the cells whose nuclei were stained with blue were examined under a fluorescence microscope and the images were recorded. Using the images obtained, the experimental groups were evaluated by comparing them with each other and with the control group.

4
RESULTS AND DISCUSSION

The aim of this study was producing polymeric nanoparticle-integrated antibacterial cryogels. To achieve this;

- Poly(4VP-co-OEGMA) random copolymer was prepared by a free-radical polymerization reaction.
- The produced poly(4VP-co-OEGMA) was cross-linked with 1,6-dibromohexane to synthesize 4VP-based cross-linked cationic nanoparticles.
- 4VP and OEGMA-500 monomers and BAAm cross-linker were used to produce 4VP-OEGMA cryogels with cryogelation.
- The produced 4VP-based cross-linked cationic nanoparticles were integrated to the 4VP-OEGMA cryogels through quaternization reaction.
- Quaternized 4VP-OEGMA cryogels were also prepared by the addition of an alkylating agent to the quaternization reaction.
- The antibacterial activity of produced cryogels were investigated against *E. coli* and *S. aureus* and their biocompatibility was tested on L929 cell line.

4.1 Characterization of the Poly(4VP-co-OEGMA) Random Copolymer

After the synthesis of poly(4VP-co-OEGMA) random copolymer with free-radical polymerization, the yield of polymerization was calculated to be 70%. The copolymer was then chemically characterized with FTIR and NMR spectroscopies and GPC.

As shown in the ^{1}H-NMR spectrum of the synthesized copolymer (Figure 4.1), a peak at 3.25 ppm was observed due to the methyl protons in the methyl ether groups found in the side chain ends of OEGMA monomer [101]. Two peaks at 8.00 and 6.35 ppm belong to the aromatic protons in the pyridine rings, in addition to a peak at 1.30 ppm that belongs to the protons of the vinyl chain of

the 4VP monomer [101], [102] were shown. The chemical composition of the synthesized copolymer was measured from the ratio of peak areas of the 4VP to OEGMA monomers to be approximately 90% and 10% mole ratio of 4VP and OEGMA monomers, respectively. Using NMR spectroscopy, all of the chemical groups in the structure of the poly(4VP-co-OEGMA) copolymer were determined and the chemical structure of the copolymer was confirmed.

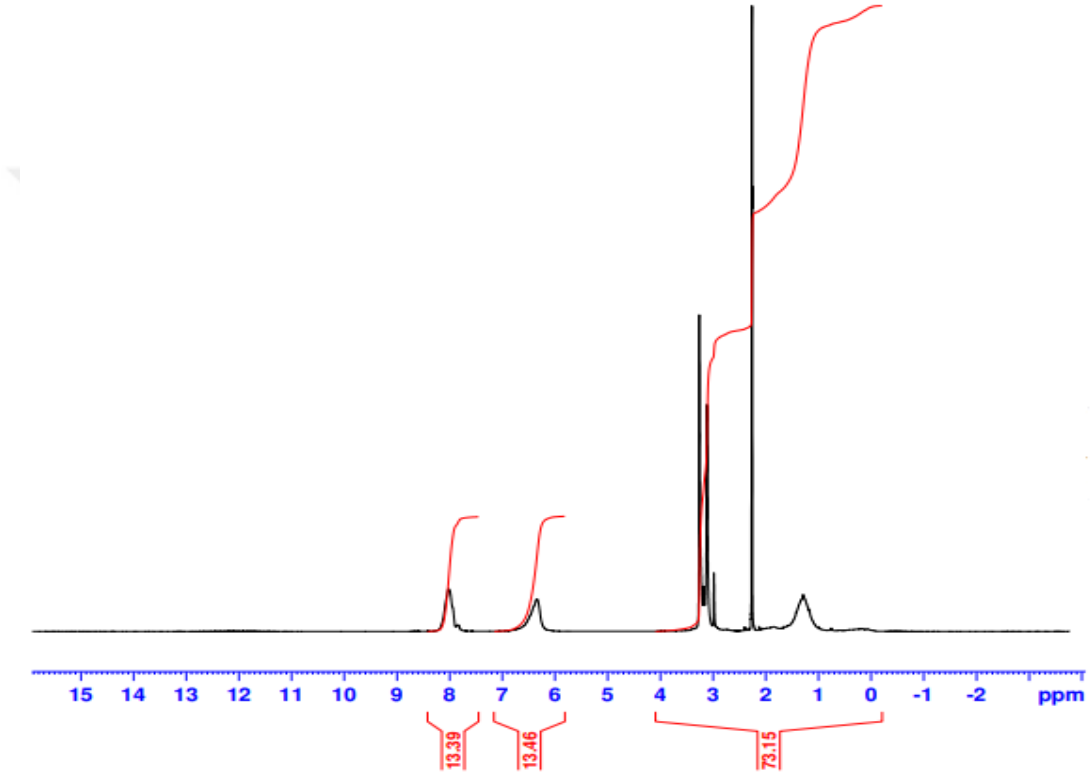

Figure 4.1 1H-NMR spectra of poly(4VP-co-OEGMA)

To further confirm the chemical structure of the copolymer, FTIR spectroscopy was used. The FTIR spectrum of the synthesized copolymer is shown in Figure 4.2. A characteristic peak at about 1600 cm^{-1} was shown due to the stretching vibration of C=N and C=C of the aromatic rings in the 4VP monomer. In addition, the peak at 1415 cm^{-1} was observed from the pyridine rings of the 4VP monomer. The peak at 1725 cm^{-1} provides the presence of the C=O group of the OEGMA-500 monomer. Moreover, the peak at 1100 cm^{-1} belonging to the C–O–C ether groups in the side chain of the OEGMA-500 monomer was shown [5].

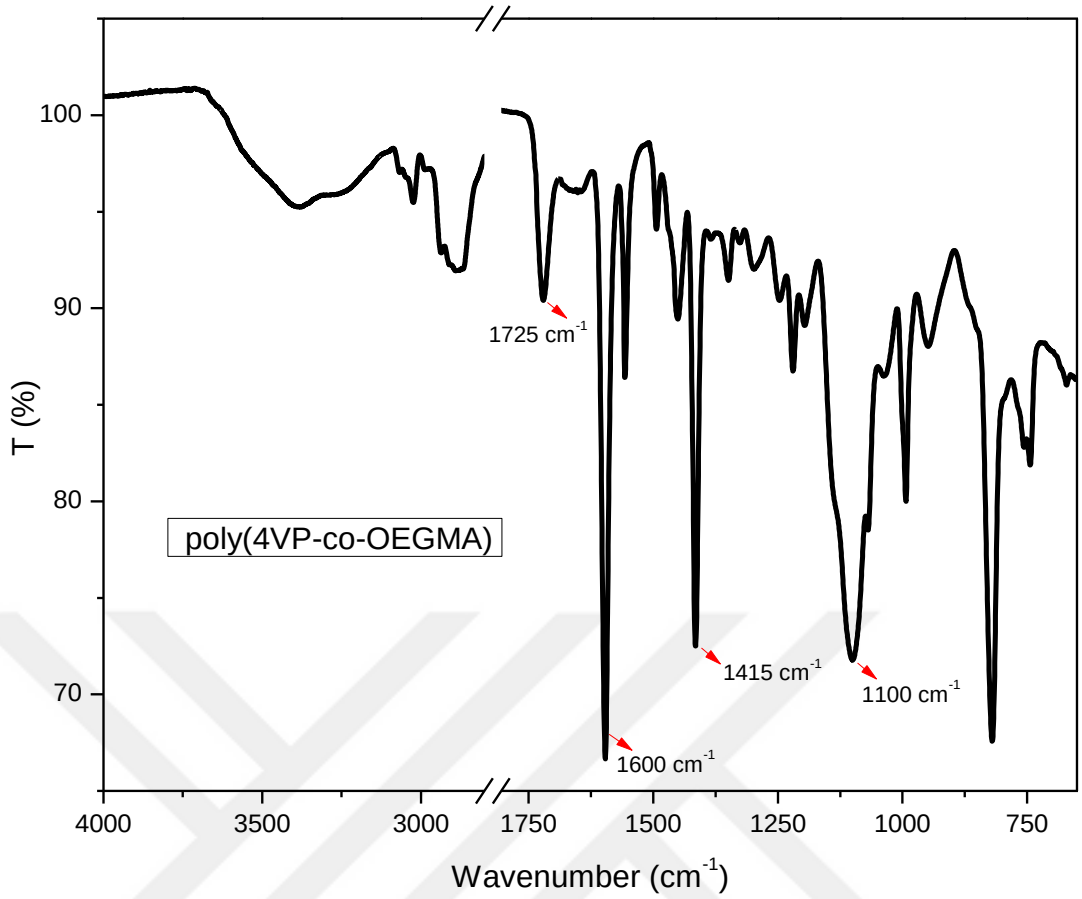

Figure 4.2 The FTIR spectrum of the synthesized poly(4VP-co-OEGMA)

The gel permeation chromatogram of the poly(4VP-co-OEGMA) copolymer is shown in Figure 4.3. The retention volume of the synthesized copolymer was determined as 2.5 mL. Also, it was found that the weight-average molecular weight of the copolymer was 39.5 kDa and its dispersity (*Đ*, M_W/M_n) value was 1.38. The peaks observed between 3.1-4.0 mL are baseline noises from the light scattering. It can be concluded that no more peaks were observed other than the copolymer's peak, which indicates that the unreacted monomers and solvent molecules were removed successfully.

These results reveal that the poly(4VP-co-OEGMA) copolymer was successfully synthesized and can be used in further steps of the study.

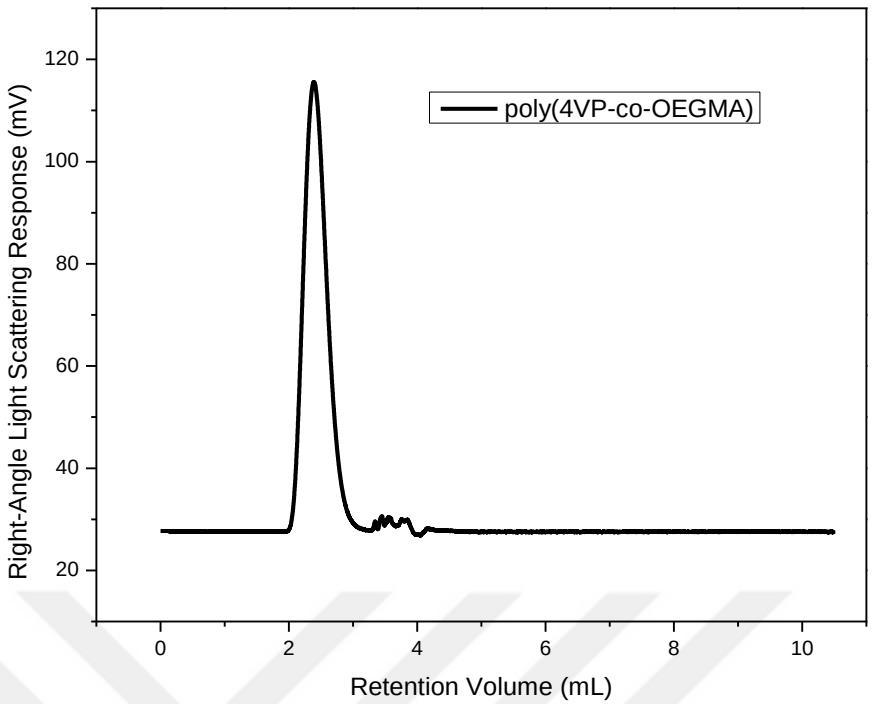

Figure 4.3 The gel permeation chromatogram of poly(4VP-co-OEGMA)

4.2 Characterization of the 4VP-Based Cross-Linked Cationic Polymeric Nanoparticles

The produced 4VP-based cross-linked cationic polymeric nanoparticles were characterized with DLS, ELS, and FTIR spectroscopies to determine their hydrodynamic diameter, zeta-potential and quaternization degree, respectively after their yield was calculated to be 66%.

FTIR spectrum of the synthesized nanoparticles is given in Figure 4.4. As the nanoparticles were produced from the previously synthesized poly(4VP-co-OEGMA) copolymer, the characteristic peaks of the copolymer at wavenumbers of 1100, 1415, 1600, and 1725 cm^{-1} were observed in the nanoparticle's spectrum as well. In addition, a new peak at 1640 $cm^{-}1$ was seen from the $C{=}N^{+}$ stretching vibration as a result of the quaternization formed from the cross-linking of the nanoparticles. The peak at 1468 cm^{-1} also indicated the quaternized pyridine rings in the 4VP monomer [5], [94]. The quaternization degree of the nanoparticles was calculated using equation (3.1) was 11%. After the chemical structure of the synthesized nanoparticles was confirmed, DLS and ELS spectroscopies were

accomplished to determine the hydrodynamic diameter and zeta-potential of the nanoparticles.

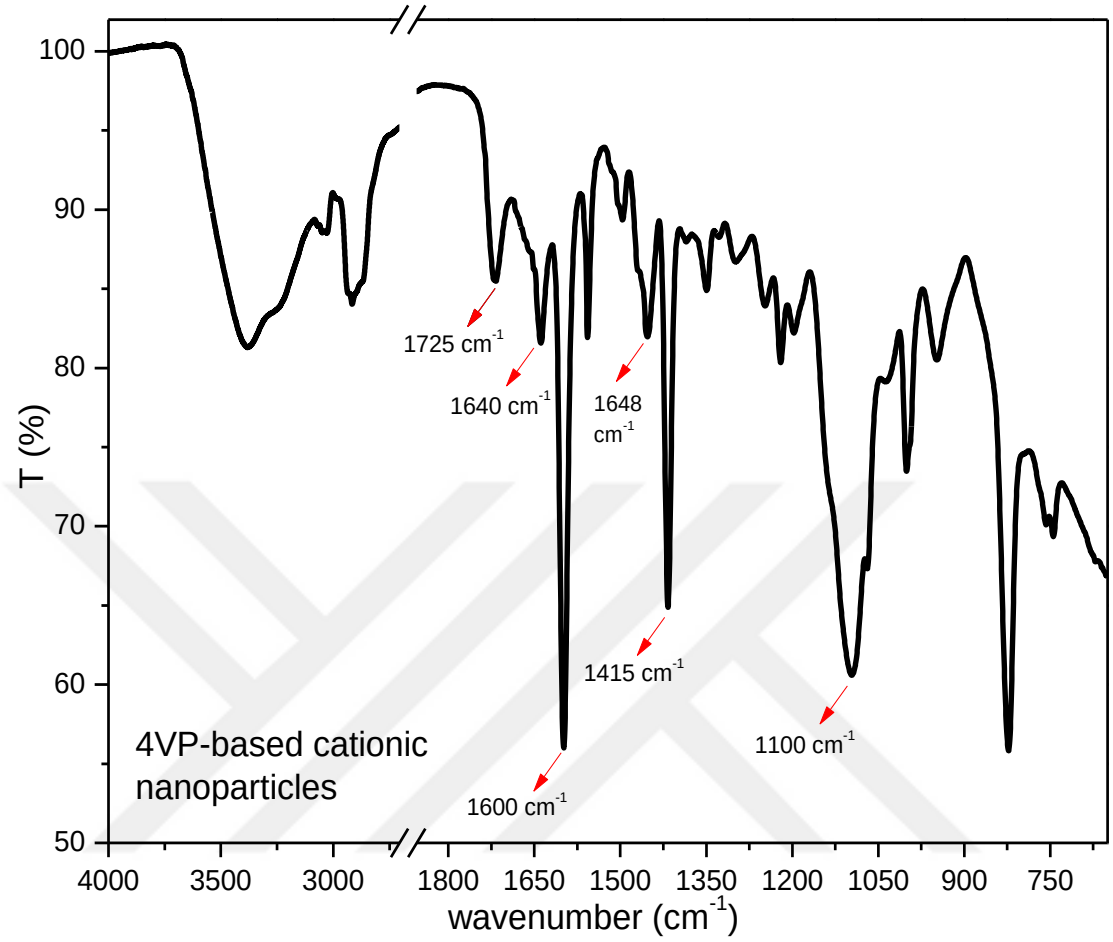

Figure 4.4 The FTIR spectrum of the synthesized 4VP-based cationic nanoparticles

The size distribution and polydispersity index of the produced nanoparticles dispersed in ultra-pure water, with concentration of 1 mg/mL were measured with DLS method, and as a result, as shown in the size distribution profile of the produced nanoparticles (Figure 4.5), the hydrodynamic diameter of the produced 4VP-based cationic nanoparticles was 112±1 nm with PdI value of 0.2.

ELS result showed that the zeta-potential of the nanoparticles was +35 mV. This is due to the positive charges on the surface of the nanoparticles as a result of the quaternization obtained from the cross-linking of poly(4VP-co-OEGMA) in the synthesis reaction of the nanoparticles.

The results indicate that positively charged nano-sized particles were successfully produced from cross-linking the poly(4VP-co-OEGMA) random copolymer.

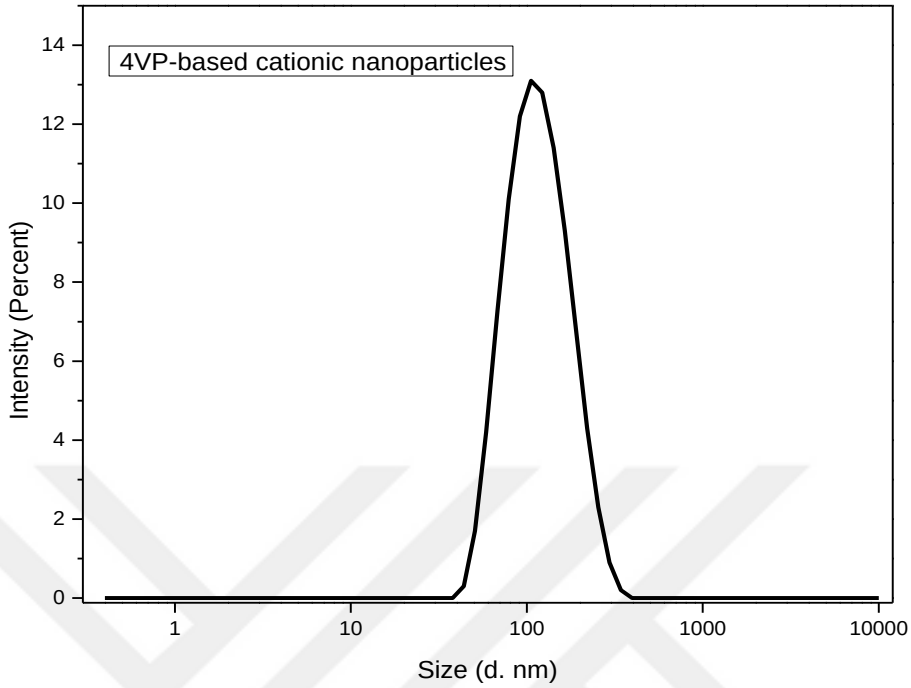

Figure 4.5 Size distribution of the 4VP-based nanoparticles

4.3 Characterization of the 4VP-OEGMA Cryogels

The synthesized non-quaternized, quaternized and nanoparticle-integrated cryogels were analyzed with FTIR spectroscopy, SEM, and texture analyzer.

The FTIR spectra of the synthesized cryogels, compared with the nanoparticles' spectrum are shown in Figure 4.6. As shown in the non-quaternized cryogel's spectrum, all the characteristic peaks of OEGMA and 4VP shown previously in the poly(4VP-co-OEGMA) and 4VP-based nanoparticles spectra were observed. In addition, a peak at wavenumber of 1650 cm^{-1} was shown due to the NH bending in BAAm. Moreover, the peak at 1640 cm^{-1} wavenumber was absent showing that there were no quaternized pyridine rings in the structure of the non-quaternized cryogel.

The spectrum of the quaternized cryogel shows all the characteristic peaks observed in the non-quaternized cryogel. On the other hand, the bands at 1415 and 1600 cm^{-1} were shown to be significantly small compared with the peaks found in the non-quaternized cryogels' spectrum. Two additional strong peaks at

wavenumbers of 1468 and 1640 cm^{-1} indicate the presence of quaternized pyridine rings in its structure. In addition, the band of BAAm at wavenumber of 1650 cm^{-1} was shown to be obscured, making a shoulder, as it was intercepted with the quaternized pyridine rings' band at 1640 cm^{-1}.

By comparing the spectra of quaternized and nanoparticle-integrated cryogels, it can be shown that there is no difference or any additional peak in the spectrum of nanoparticle-integrated cryogel, as all the chemical bonds found in the integrated nanoparticles' structure are found also in the structure of quaternized cryogels. In addition, using the FTIR results, the quaternization degrees of both the quaternized as well as the nanoparticle-integrated cryogels were calculated to be 80%.

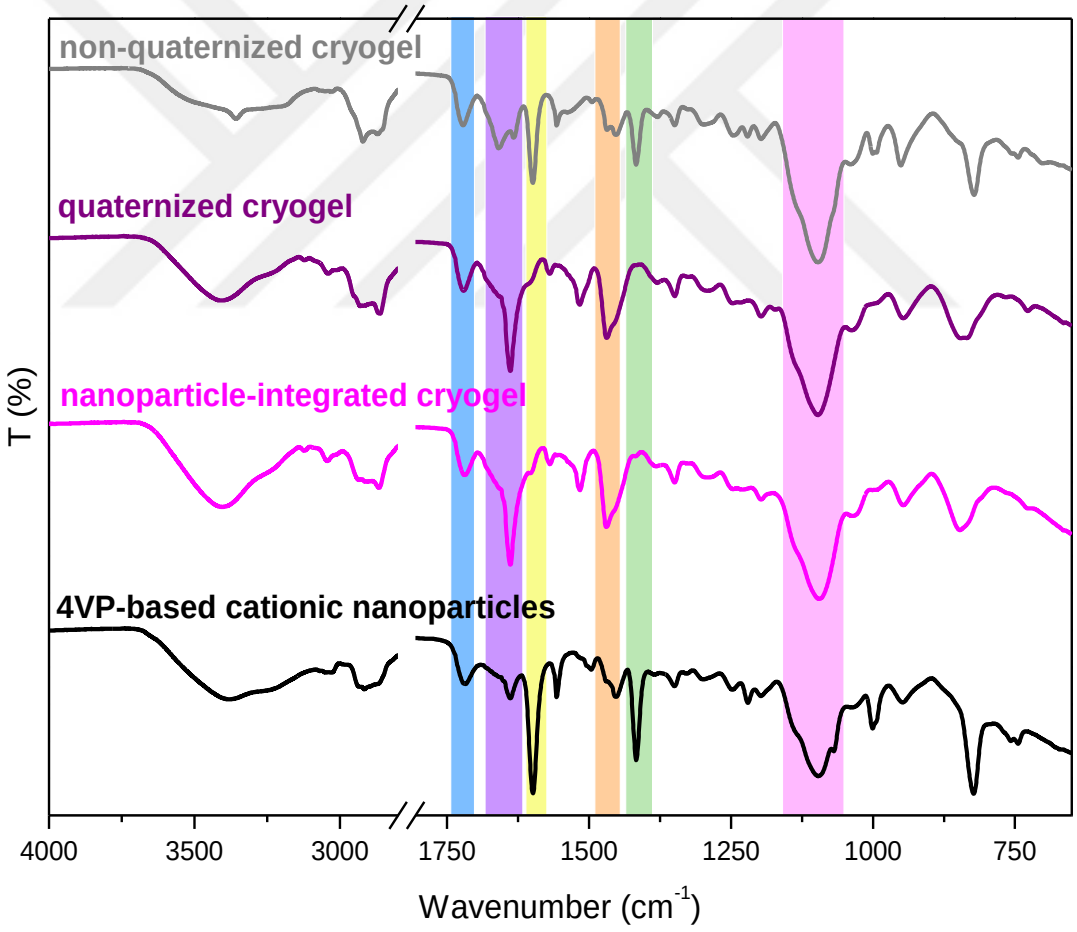

Figure 4.6 FTIR spectra of the synthesized 4VP-based cationic nanoparticles, and the non-quaternized, quaternized, and nanoparticle-integrated cryogels

After the chemical structure of the synthesized cryogels was analyzed and confirmed, SEM images for dried cryogel's cross-sections were taken to investigate their pore structure and to ensure the attachment of the nanoparticles on the pore walls of the nanoparticle-integrated cryogels. The SEM images of the synthesized non-quaternized, quaternized, and nanoparticle-integrated cryogels, at 500X and 20,000X magnifications, were shown in Figure 4.7, in which, highly interconnected macroporous cryogels with average pore size of 50 μm were observed. In addition, the integrated nanoparticles were shown clearly to be attached to the pore gel wall. While the non-quaternized and quaternized cryogels were not having any particles on their surfaces.

As shown in Figure 4.7, the interconnected pores in the nanoparticle-integrated cryogel were more irregular compared with the non-quaternized and quaternized cryogels, even though their average pore size was the same. This feature might be an advantage when using in biomedical applications, such as tissue engineering. While smaller pores offer high surface area for cell adhesion, larger pores promote cell migration and diffusion [24]. Larger pores are necessary also for the transmission of oxygen and nutrients to the proliferating cells [103].

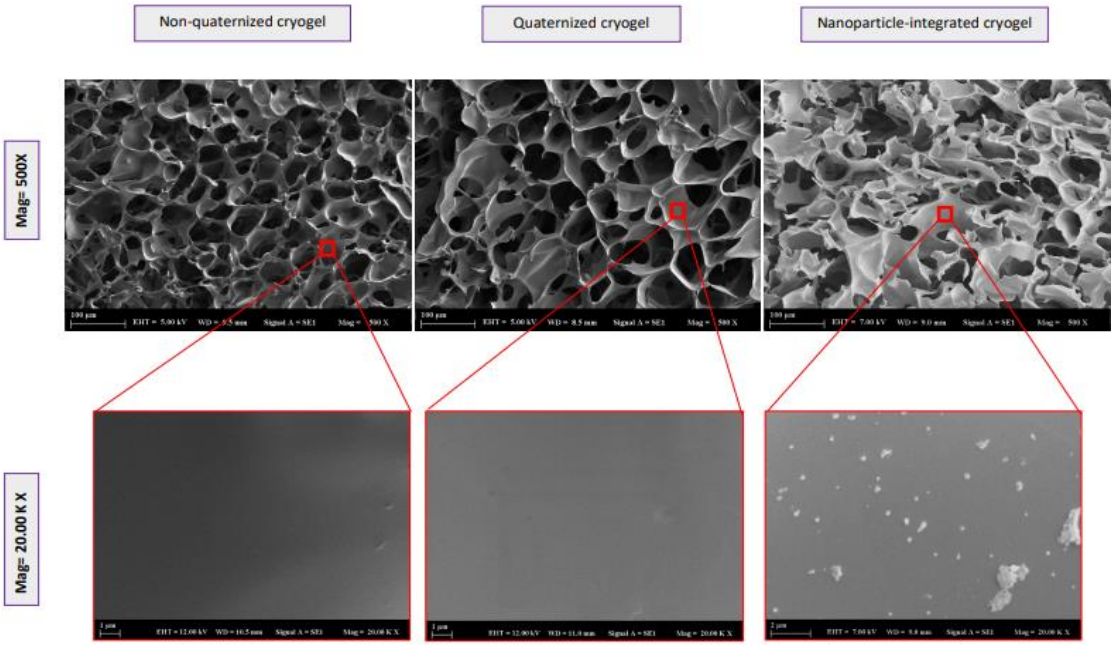

Figure 4.7 SEM images of non-quaternized, quaternized and nanoparticle-integrated cryogels at 500 X and 20,000 X magnifications

The swelling behavior of the produced cryogels was investigated by swelling the dry cryogels in ultra-pure water. The weight and volume fractions were calculated using equations (3.2) and (3.3) and plotted. As shown in Figure 4.8, the weight fraction after 4 hours of the non-quaternized cryogel was 15.43, whereas when the quaternization degree of the cryogel increased to 80%, the weight fraction increased to 22.60. When compared with the quaternized cryogel, nanoparticle-integrated cryogel was showing lower weight fraction (12.03), which might be a result of structural changes occurred during the quaternization reaction due to the addition of secondary cross-linker. The volume swelling fractions of the non-quaternized, quaternized, and nanoparticle-integrated cryogels were 1.61, 1.90, and 1.37 respectively.

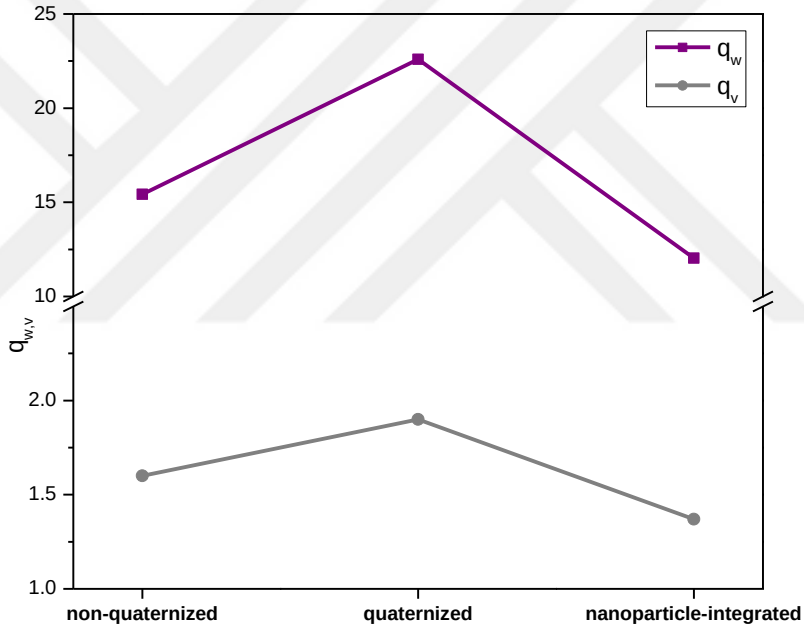

Figure 4.8 Swelling fractions of non-quaternized, quaternized and nanoparticle-integrated cryogels

The synthesized cryogels show remarkably high weight fractions compared with their volume fractions. The difference between weight and volume fractions gives information about the porosity of the cryogels. As shown in Figure 4.8, the quaternized cryogel shows larger porosity after swelling compared to the non-quaternized and nanoparticle-integrated cryogels even though the SEM images of the dry cryogels show approximately the same pore size of all the produced cryogels. This is due to their very high swelling capacity as a result of the positively

charged pyridine rings in the structure of quaternized-cryogels, where charged cryogels absorb more water than neutral cryogels as their hydrophilicity increases when they are charged [104]. Thus, their swelling increases as well when increasing their positive charges [104], [105]. Although the nanoparticle-integrated cryogels have the same quaternization degree of the quaternized cryogels, they did not show the same swelling behavior. This might be a result of the addition of the secondary cross-linker, 1,6-dibromohexane, which might have affected their pores' structure, where the addition of nanoparticles should not significantly change the swelling of the cryogels [24].

The swelling kinetics illustrated in Figure 4.9 shows the super-fast swelling of the produced non-quaternized and quaternized cryogels in less than one minute as shown in Figure 4.9. Although non-quaternized and quaternized cryogels reach their equilibrium swelling state in less than 1 minute, it was observed that the nanoparticle-integrated cryogel kept swelling after 4 hours. In addition, non-quaternized and quaternized cryogels showed more rapid swelling, in 10 and 20 seconds, respectively. Nanoparticle-integrated cryogel showed slower swelling compared to both non-quaternized and quaternized cryogels.

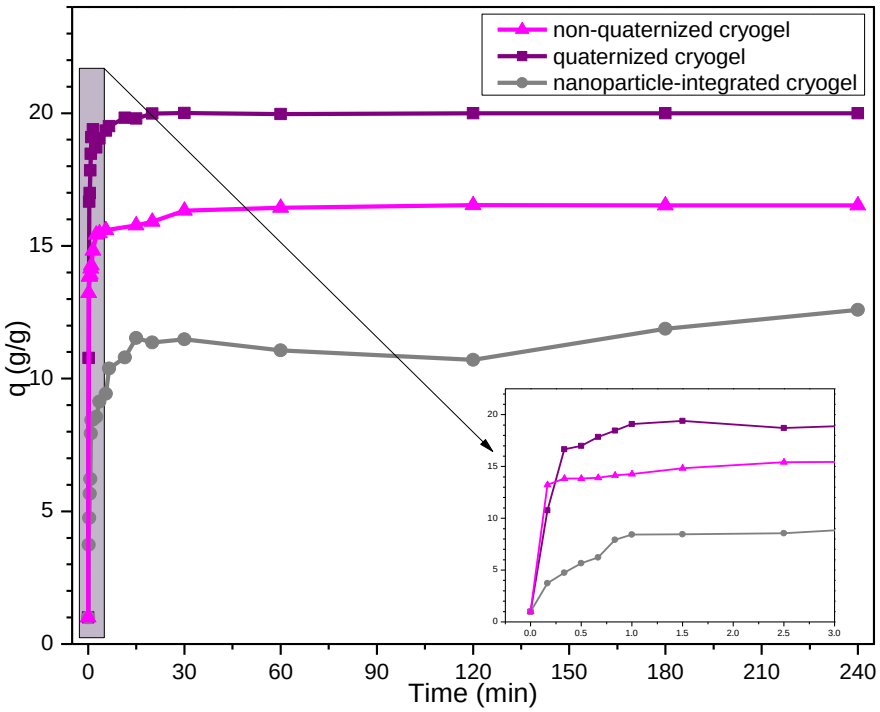

Figure 4.9 Swelling kinetics of non-quaternized, quaternized, and nanoparticle-integrated cryogels after 4 hours

To examine the reason behind the slower swelling of the nanoparticle-integrated cryogel, a quaternized cryogel with 75% quaternization degree containing both 1-bromohexane and the secondary cross-linker (1,6-dibromohexane) was prepared. When the swelling kinetics of this secondary cross-linked cryogel was examined, it was observed that its weight swelling fraction was 13.47, as shown in Figure 4.10, which is very similar to the nanoparticle-integrated cryogel that has also 1,6-dibromohexane in its structure. In addition, the secondary cross-linked cryogel have shown slow swelling, similar to the nanoparticle-integrated cryogel, when compared to the non-quaternized and quaternized cryogels. As a result, it can be said that the addition of 1,6-dibromohexane to covalently integrate nanoparticles to the cryogels not only attached the nanoparticles to the cryogel, but also secondarily cross-linked the cryogel and decreased its swelling.

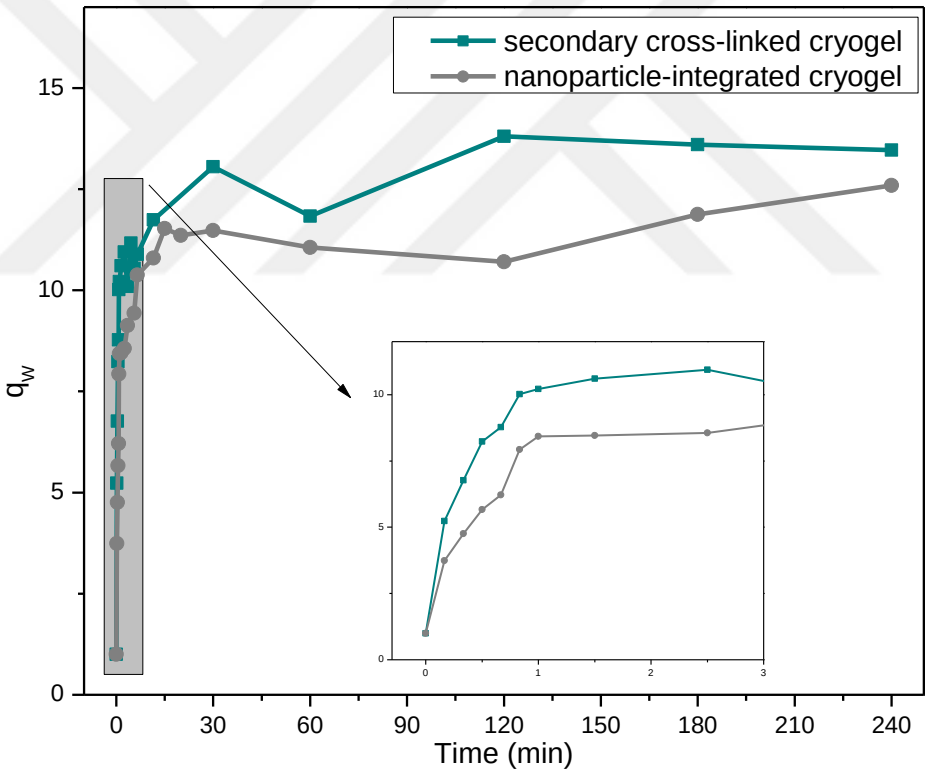

Figure 4.10 Swelling kinetics of nanoparticle-integrated cryogel compared with secondary cross-linked cryogel

The synthesized cryogels showed good mechanical properties as shown in Figure 4.11, where images for the initial, compressed, and recovery states of the synthesized 4VP-OEGMA cryogel were taken. As shown in Figure 4.11, the

synthesized cryogel was compression-resistant as the cryogel return to its initial state and fully recovered after relaxation by immediately absorbing the squeezed water again showing high elasticity, similar to other cryogels [99], [106].

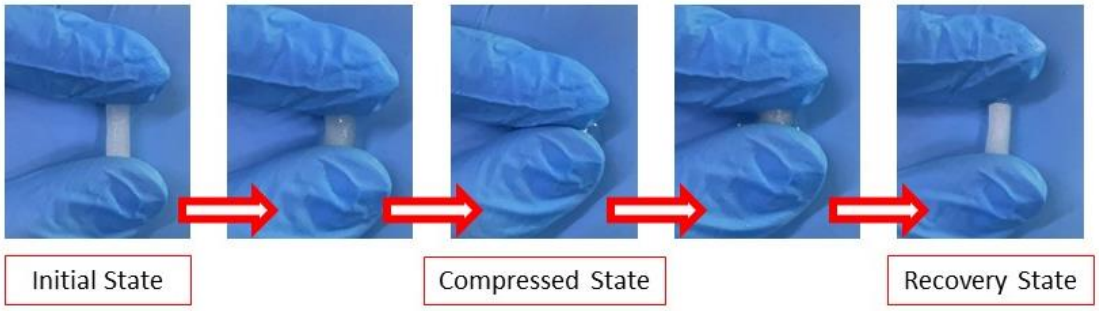

Figure 4.11 The compression resistance of the synthesized cryogel

4.4 Antibacterial Activity of the Synthesized Cryogels

The antibacterial activity of the non-quaternized, quaternized and nanoparticle-integrated cryogels were determined against *S. aureus* and *E. coli*. The results were evaluated through colony numbers (Table 4.2) and shown in percent (%) kill (Figure 4.12) and log reduction (Figure 4.13). Non-quaternized cryogel exhibited antibacterial activity on both *S. aureus* (1.04-log reduction or 90.0 % kill) and *E. coli* (0.91-log reduction or 87.8 % kill). The quaternized cryogel displayed higher antibacterial activity against both *E. coli* and *S. aureus*. 1.12-log reduction or 92.42 % kill on *S. aureus* and 2.48-log reduction or 99.6 % kill on *E. coli* were observed. However, nanoparticle-integrated cryogel displayed antibacterial activity on *E. coli* (1.25-log reduction or 94.41 % kill), but on *S. aureus* (0.36-log reduction or 56.06 % kill), exhibited low antibacterial activity. Considering all the results, quaternized cryogel, which has the antibacterial property, exhibited the greatest activity by maintaining its antibacterial effect for 4 hours. Therefore, these findings represent that the antibacterial activity increases significantly with the quaternization of the cryogel and the effect of the nanoparticle-integrated cryogel is higher on gram negative bacteria.

Table 4.2 Images of petri dishes (10^{-4} dilution) after bacteria incubation of control, non-quaternized, quaternized and nanoparticle-integrated cryogels

Sample	*E. coli*	*S. aureus*
Control	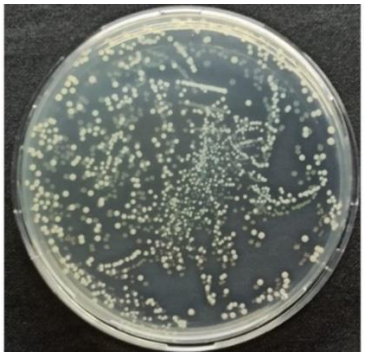	
Non-quaternized cryogel		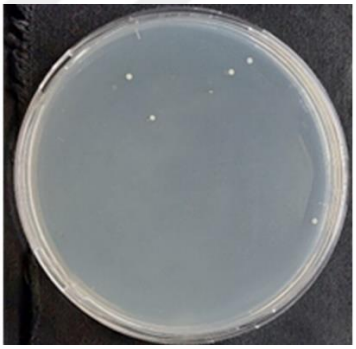
Quaternized cryogel	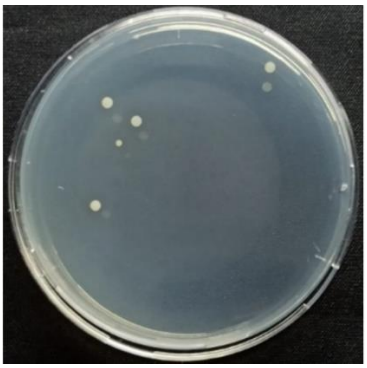	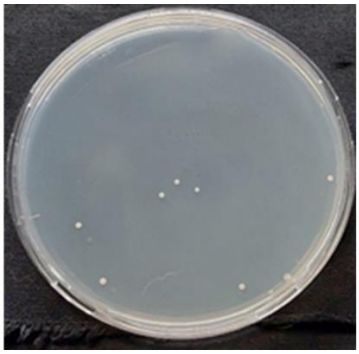
Nanoparticle-integrated cryogel	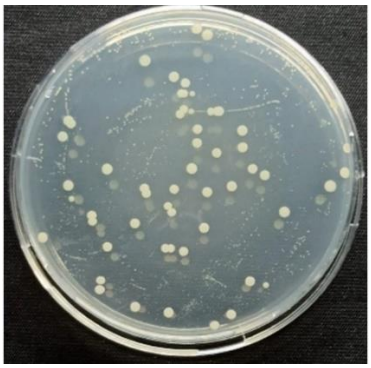	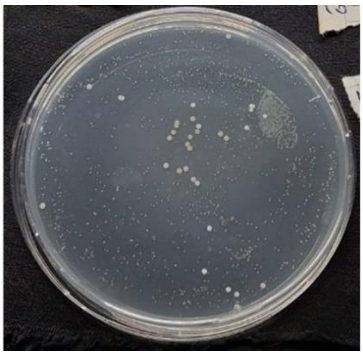

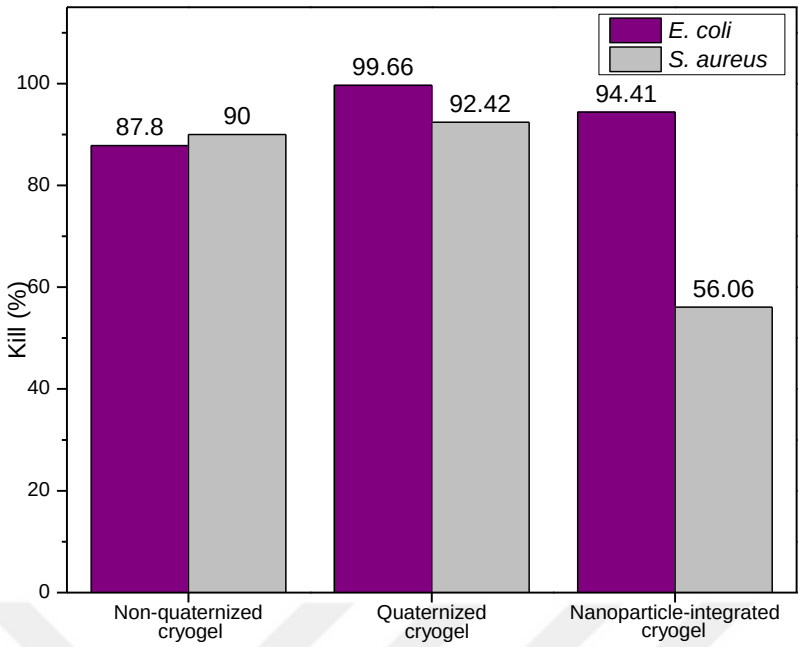

Figure 4.12 % kill of *E. coli* and *S. aureus* on non-quaternized, quaternized and nanoparticle-integrated cryogels at 4 hours

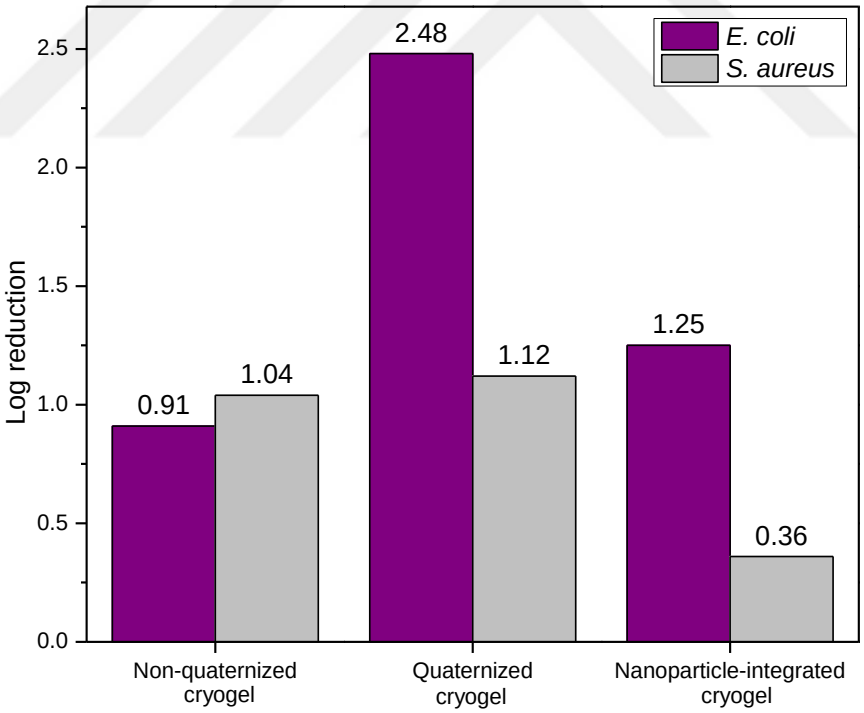

Figure 4.13 Log reduction of *S. aureus* and *E. coli* on non-quaternized, quaternized and nanoparticle-integrated cryogels at 4 hours

Although the antibacterial activity of the nanoparticle-integrated cryogel was not very high against gram positive bacteria *(S. aureus)*, when this cryogel was

analyzed with SEM after 4 hours of incubation with bacteria, as shown in Figure 4.14, damaged *S. aureus* were observed clearly on its pore walls. The SEM analysis validated the presence of both the 1 μm sized *S. aureus* with extensively damaged membrane in addition to the integrated nanoparticles on the surface of the cryogel proving the effect of nanoparticle-integrated cryogels against gram positive bacteria as well. The morphology of the observed damaged *S. aureus* on the cryogel were similar to the damaged bacteria images in literature [107], [108].

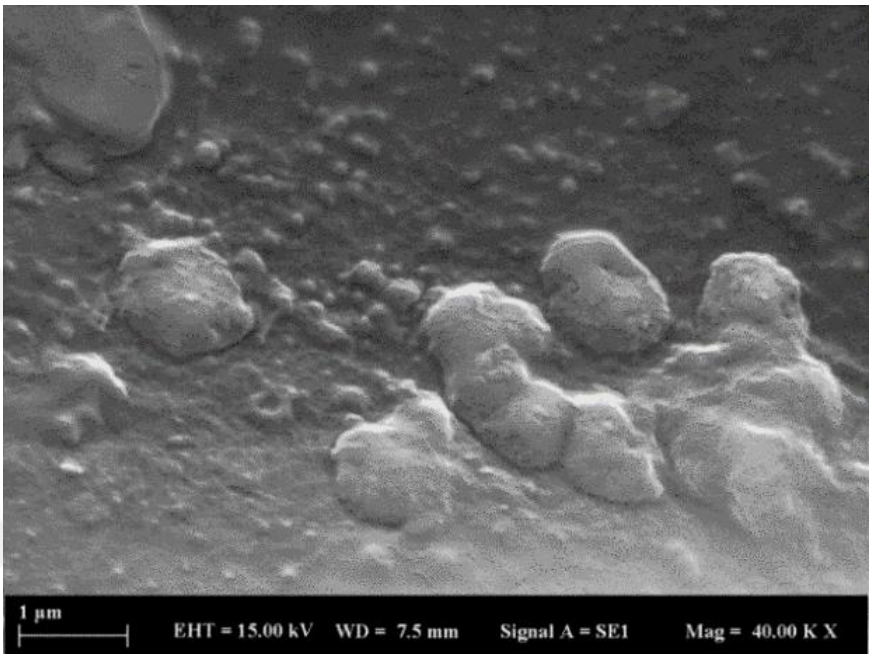

Figure 4.14 SEM image of damaged *S. aureus* on the pore wall of nanoparticle-integrated cryogel at 40,000 X magnification

4.5 Biocompatibility Tests

Cytotoxicity of non-quaternized, quaternized, and nanoparticle-integrated cryogels were analyzed using the MTT method after treatment with L929 fibroblast cells. As a result of this analysis, cell viability percentages were obtained as 99.06%, 96.2% and 92.6%, for the non-quaternized, quaternized, and nanoparticle-integrated cryogels, respectively, when compared to the control group (Figure 4.15). Although the homopolymers of QP4VP have cytotoxic effects, copolymers of QP4VP can be biocompatible by including hydrophilic and biocompatible monomers into the polymer chain as shown in the study of Stratton et al. in which quaternized antibacterial copolymers produced from 4VP and

PEGMA monomers showed high biocompatibility when they were tested on Caco-2, a human intestinal epithelial cell line [109]. As a result, all the produced 4VP-based cryogels were biocompatible due to the presence of OEGMA groups in their structure.

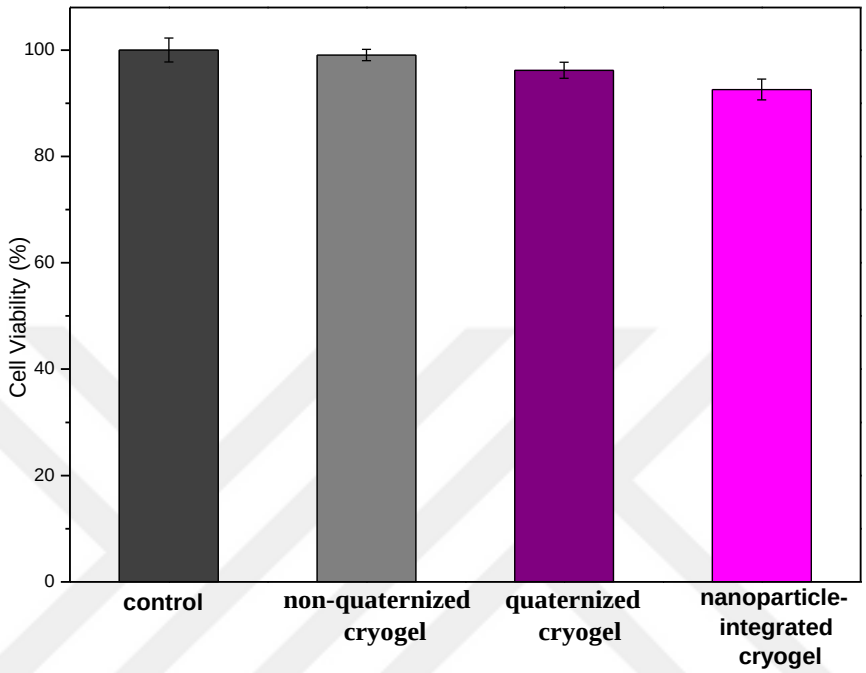

Figure 4.15 Cell viability analysis data on L929 fibroblast cells of control, non-quaternized, quaternized and nanoparticle-integrated groups

DAPI staining was performed to examine the effect of the produced cryogels on cell density and adhesion. Cells that adhered were visualized after staining under a fluorescence microscope. In the images (Figure 4.16), it was obtained that the density of the cells to which non-quaternized, quaternized and nanoparticle-integrated cryogels were applied was higher than the control group, and at the same time, when the groups were compared among themselves, the cell densities were determined, from highest to lowest, as nanoparticle-integrated, quaternized, and non-quaternized, respectively, where it was previously proved that positively charged macroporous hydrogels have a greater tendency for cell adhesion [30], [110].

For instance, in the study of Janouskova et al. the positively charged quaternary ammonium groups outperform all of the negatively charged, neutral, and

zwitterionic groups in cell attachment and proliferation significantly in the modified macroporous poly(HEMA)-based hydrogels [111].

In another study, modified acrylated-PVA-based macroporous hydrogels containing 2-(diethylamino) ethylmethacrylate (positively charged) and acrylic acid (negatively charged) monomers were prepared and it was shown that the positively charged hydrogels containing 2-(diethylamino) ethylmethacrylate monomers were superior to the unmodified and acrylic acid-containing negatively charged hydrogels for cell adherence and spreading on both L929 and human mesenchymal stem cells (hMSC) [112].

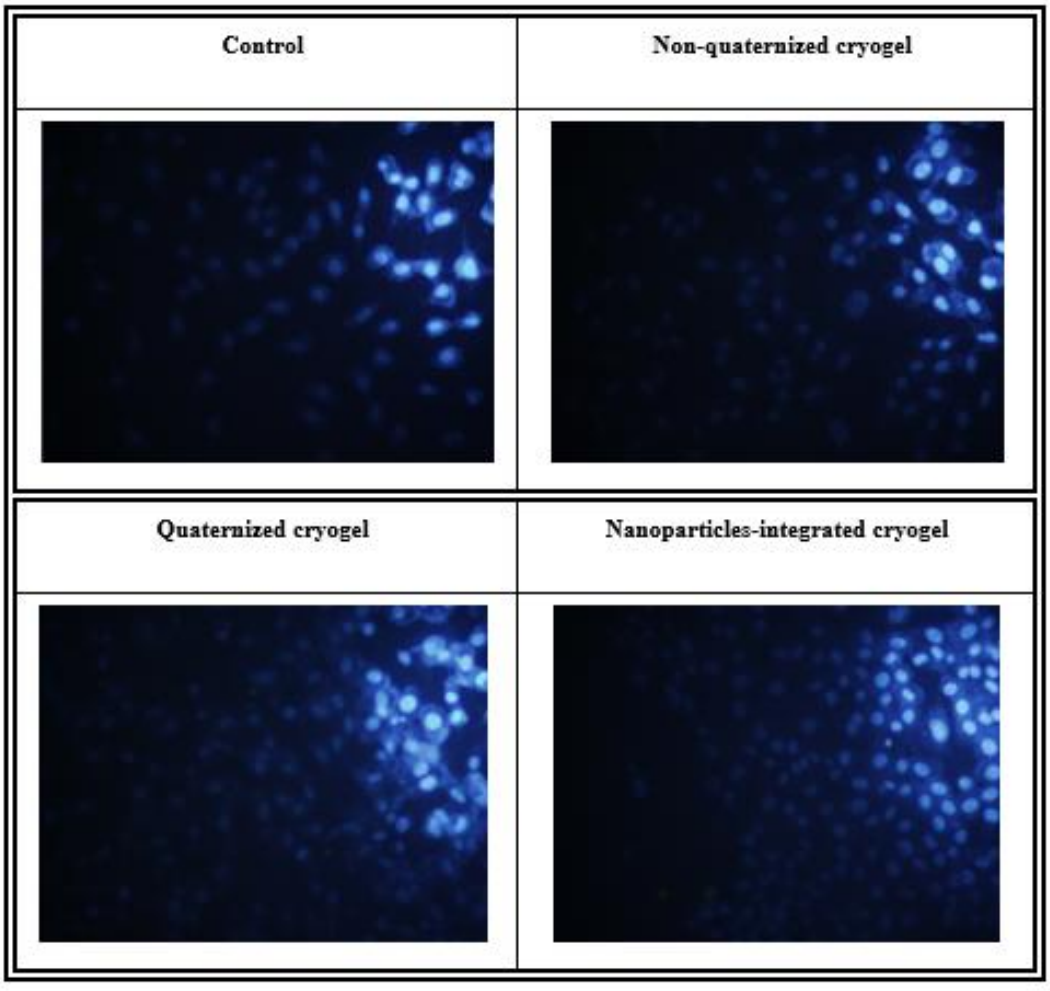

Figure 4.16 Fluorescence microscope images (40X) of DAPI-stained L929 cells after incubation with the produced cryogels

4.6 Conclusion

In this study, for the first time, cationic polymeric nanoparticle-integrated antibacterial cryogels were prepared from 4VP and OEGMA monomers. As a result of the experiments carried out in this study, the following conclusions can be drawn:

- Poly(4VP-co-OEGMA) random copolymer was prepared by free-radical polymerization of 4VP and OEGMA monomers and the characterization results from NMR and FTIR spectroscopies showed that poly(4VP-co-OEGMA) was synthesized successfully with 90% 4VP and 10% OEGMA content.
- 4VP-based cationic nanoparticles were obtained from cross-linking the previously prepared copolymer with a bi-functional group, 1,6-dibromohexane. It was revealed that monodisperse 4VP-based cationic nanoparticles with hydrodynamic diameter of 112±1 nm and zeta potential of +35 mV were successfully synthesized.
- 4VP-OEGMA cryogels were produced from cryogelation of 4VP and OEGMA monomers with BAAm cross-linker. Then, the nanoparticle-integrated cryogels and quaternized cryogels were produced through quaternization reaction for antibacterial purposes.
- FTIR spectra of the produced cryogels showed that the quaternization degree of both quaternized and nanoparticle-integrated cryogels were 80%. In addition, FTIR spectra revealed the successful preparation of all the cryogels.
- SEM images illustrated that the cryogels have macroporous interconnected microstructure with pore size of 50 μm. Moreover, it was clearly shown in the SEM images of the nanoparticle-integrated cryogels that the nanoparticles have successfully attached to the pore walls of the cryogels.
- Swelling studies for the prepared 4VP-OEGMA cryogels showed their super-fast swelling in less than one minute for all the samples.
- All of the produced cryogels have shown antibacterial activity against both gram negative and gram positive bacteria. Quaternized cryogel, exhibited

the highest activity by maintaining its antibacterial effect for 4 hours against both *E. coli* and *S. aureus* with 99.6% and 92.42% kill, respectively whereas the non-quaternized cryogels showed 90.0 % kill against *S. aureus* and 87.8 % kill against *E. coli*. Nanoparticle-integrated cryogels showed great antibacterial activity against gram negative bacteria, *E. coli* with 94.41% kill after 4 hours.

- Cytotoxicity test of the cryogels on L929 cell line showed that all the samples are biocompatible with cell viability of 99.06%, 96.2% and 92.6% for non-quaternized, quaternized and nanoparticle-integrated cryogels, respectively.
- The DAPI staining study displayed that the cryogels were adhered on L929 fibroblast cell lines. The cell densities were shown to be, from highest to lowest, as nanoparticle-integrated, quaternized, and non-quaternized cryogels, respectively.

Considering the findings in the thesis study, it was shown that the prepared 4VP-based cross-linked cationic nanoparticle-integrated 4VP-OEGMA cryogels have sufficient antibacterial activity especially against gram negative bacteria. Thus, it can be concluded that the produced cryogels have the potential to be used as wound dressing and in other biomedical applications.

Further studies are planned to examine the effect of the quaternization degree and nanoparticles concentration on the antibacterial activity of nanoparticle-integrated cryogel. In addition, in order to use the produced cryogels in tissue engineering applications, such as wound dressing, further studies, such as oxygen permeability and wound healing should be tested to ensure that the produced biomaterials are able to be used in such applications. Moreover, in order to further control the cryogelation reaction and to obtain more homogeneous-structured cryogel, the reaction is planned to be done under isothermal conditions, where inhibitor can be added to the cryogels solution to delay the cryogelation, or initial precursor solution can be quenched in liquid nitrogen.

REFERENCES

[1] C. Deusenbery, Y. Wang, and A. Shukla, "Recent Innovations in Bacterial Infection Detection and Treatment," *ACS Infect. Dis.*, vol. 7, no. 4, pp. 695–720, Apr. 2021, doi: 10.1021/acsinfecdis.0c00890.

[2] B. Aslam *et al.*, "Antibiotic resistance: a rundown of a global crisis," *Infect Drug Resist*, vol. 11, pp. 1645–1658, Oct. 2018, doi: 10.2147/IDR.S173867.

[3] M. Boulos, T. Bassal, A. Layyous, M. Basheer, and N. Assy, "Inflammation in COVID-19: A Risk for Superinfections," *COVID*, vol. 2, no. 11, Art. no. 11, Nov. 2022, doi: 10.3390/covid2110116.

[4] A. M. Carmona-Ribeiro and L. D. De Melo Carrasco, "Cationic Antimicrobial Polymers and Their Assemblies," *International Journal of Molecular Sciences*, vol. 14, no. 5, Art. no. 5, May 2013, doi: 10.3390/ijms14059906.

[5] D. Gokkaya, M. Topuzogullari, T. Arasoglu, K. Trabzonlu, M. M. Ozmen, and S. Abdurrahmanoğlu, "Antibacterial properties of cationic copolymers as a function of pendant alkyl chain length and degree of quaternization," *Polym Int*, vol. 70, no. 6, pp. 829–836, Jun. 2021, doi: 10.1002/pi.6170.

[6] A. Jain, L. S. Duvvuri, S. Farah, N. Beyth, A. J. Domb, and W. Khan, "Antimicrobial polymers," *Adv Healthc Mater*, vol. 3, no. 12, pp. 1969–1985, Dec. 2014, doi: 10.1002/adhm.201400418.

[7] N. Nasri *et al.*, "Past and Current Progress in the Development of Antiviral/Antimicrobial Polymer Coating towards COVID-19 Prevention: A Review," *Polymers*, vol. 13, p. 4234, Dec. 2021, doi: 10.3390/polym13234234.

[8] B. Bechinger and S.-U. Gorr, "Antimicrobial Peptides: Mechanisms of Action and Resistance," *J Dent Res*, vol. 96, no. 3, pp. 254–260, Mar. 2017, doi: 10.1177/0022034516679973.

[9] E. Sánchez-López *et al.*, "Metal-Based Nanoparticles as Antimicrobial Agents: An Overview," *Nanomaterials (Basel)*, vol. 10, no. 2, p. 292, Feb. 2020, doi: 10.3390/nano10020292.

[10] M. Bakhshpour, N. Idil, I. Perçin, and A. Denizli, "Biomedical Applications of Polymeric Cryogels," *Applied Sciences*, vol. 9, no. 3, Art. no. 3, Jan. 2019, doi: 10.3390/app9030553.

[11] X. Zhang *et al.*, "The fabrication of antibacterial hydrogels for wound healing," *European Polymer Journal*, vol. 146, p. 110268, Mar. 2021, doi: 10.1016/j.eurpolymj.2021.110268.

[12] B. Akin and M. M. Ozmen, "Antimicrobial cryogel dressings towards effective wound healing," *Prog Biomater*, vol. 11, no. 4, pp. 331–346, Dec. 2022, doi: 10.1007/s40204-022-00202-w.

[13] S. J. Shirbin *et al.*, "Polypeptide-Based Macroporous Cryogels with Inherent Antimicrobial Properties: The Importance of a Macroporous Structure," *ACS*

Macro Lett., vol. 5, no. 5, pp. 552–557, May 2016, doi: 10.1021/acsmacrolett.6b00174.

[14] Y. Saylan and A. Denizli, "Supermacroporous Composite Cryogels in Biomedical Applications," *Gels*, vol. 5, no. 2, p. E20, Apr. 2019, doi: 10.3390/gels5020020.

[15] K. R. Hixon, T. Lu, and S. A. Sell, "A comprehensive review of cryogels and their roles in tissue engineering applications," *Acta Biomater*, vol. 62, pp. 29–41, Oct. 2017, doi: 10.1016/j.actbio.2017.08.033.

[16] L. Yao *et al.*, "A shape memory and antibacterial cryogel with rapid hemostasis for noncompressible hemorrhage and wound healing," *Chemical Engineering Journal*, vol. 428, p. 131005, Jan. 2022, doi: 10.1016/j.cej.2021.131005.

[17] S. Sezen, V. K. Thakur, and M. M. Ozmen, "Highly Effective Covalently Crosslinked Composite Alginate Cryogels for Cationic Dye Removal," *Gels*, vol. 7, no. 4, Art. no. 4, Dec. 2021, doi: 10.3390/gels7040178.

[18] İ. A. İşoğlu, C. Demirkan, M. G. Şeker, K. Tuzlakoğlu, and S. D. İşoğlu, "Antibacterial Bilayered Skin Patches Made of HPMA and Quaternary Poly(4-vinyl pyridine)," *Fibers Polym*, vol. 19, no. 11, pp. 2229–2236, Nov. 2018, doi: 10.1007/s12221-018-8480-9.

[19] S.-L. Loo *et al.*, "Superabsorbent Cryogels Decorated with Silver Nanoparticles as a Novel Water Technology for Point-of-Use Disinfection," *Environ. Sci. Technol.*, vol. 47, no. 16, pp. 9363–9371, Aug. 2013, doi: 10.1021/es401219s.

[20] E. K. Radwan, M. E. El-Naggar, A. Abdel-Karim, and A. R. Wassel, "Multifunctional 3D cationic starch/nanofibrillated cellulose/silver nanoparticles nanocomposite cryogel: Synthesis, adsorption, and antibacterial characteristics," *International Journal of Biological Macromolecules*, vol. 189, pp. 420–431, Oct. 2021, doi: 10.1016/j.ijbiomac.2021.08.108.

[21] K. Erol, M. Bolat, D. Tatar, C. Nigiz, and D. A. Köse, "Synthesis, characterization and antibacterial application of silver nanoparticle embedded composite cryogels," *Journal of Molecular Structure*, vol. 1200, p. 127060, Jan. 2020, doi: 10.1016/j.molstruc.2019.127060.

[22] H. Ye, J. Cheng, and K. Yu, "In situ reduction of silver nanoparticles by gelatin to obtain porous silver nanoparticle/chitosan composites with enhanced antimicrobial and wound-healing activity," *International Journal of Biological Macromolecules*, vol. 121, pp. 633–642, Jan. 2019, doi: 10.1016/j.ijbiomac.2018.10.056.

[23] R. Chen, Q. Chen, D. Huo, Y. Ding, Y. Hu, and X. Jiang, "In situ formation of chitosan-gold hybrid hydrogel and its application for drug delivery," *Colloids Surf B Biointerfaces*, vol. 97, pp. 132–137, Sep. 2012, doi: 10.1016/j.colsurfb.2012.03.027.

[24] N. Sahiner, S. Sagbas, M. Sahiner, and C. Silan, "P(TA) macro-, micro-, nanoparticle-embedded super porous p(HEMA) cryogels as wound dressing

material," *Materials Science and Engineering: C*, vol. 70, pp. 317–326, Jan. 2017, doi: 10.1016/j.msec.2016.09.025.

[25] E. M. Ahmed, "Hydrogel: Preparation, characterization, and applications: A review," *Journal of Advanced Research*, vol. 6, no. 2, pp. 105–121, Mar. 2015, doi: 10.1016/j.jare.2013.07.006.

[26] I. N. Savina, M. Zoughaib, and A. A. Yergeshov, "Design and Assessment of Biodegradable Macroporous Cryogels as Advanced Tissue Engineering and Drug Carrying Materials," *Gels*, vol. 7, no. 3, p. 79, Jun. 2021, doi: 10.3390/gels7030079.

[27] M. Bahram, N. Mohseni, M. Moghtader, M. Bahram, N. Mohseni, and M. Moghtader, *An Introduction to Hydrogels and Some Recent Applications*. IntechOpen, 2016. doi: 10.5772/64301.

[28] I. P. Harrison and F. Spada, "Hydrogels for Atopic Dermatitis and Wound Management: A Superior Drug Delivery Vehicle," *Pharmaceutics*, vol. 10, no. 2, Art. no. 2, Jun. 2018, doi: 10.3390/pharmaceutics10020071.

[29] K. Varaprasad, G. M. Raghavendra, T. Jayaramudu, M. M. Yallapu, and R. Sadiku, "A mini review on hydrogels classification and recent developments in miscellaneous applications," *Materials Science and Engineering: C*, vol. 79, pp. 958–971, Oct. 2017, doi: 10.1016/j.msec.2017.05.096.

[30] Y. Ma, X. Wang, T. Su, F. Lu, Q. Chang, and J. Gao, "Recent Advances in Macroporous Hydrogels for Cell Behavior and Tissue Engineering," *Gels*, vol. 8, no. 10, Art. no. 10, Oct. 2022, doi: 10.3390/gels8100606.

[31] K. J. De France, F. Xu, and T. Hoare, "Structured Macroporous Hydrogels: Progress, Challenges, and Opportunities," *Advanced Healthcare Materials*, vol. 7, no. 1, p. 1700927, 2018, doi: 10.1002/adhm.201700927.

[32] N. Annabi *et al.*, "Controlling the porosity and microarchitecture of hydrogels for tissue engineering," *Tissue Eng Part B Rev*, vol. 16, no. 4, pp. 371–383, Aug. 2010, doi: 10.1089/ten.TEB.2009.0639.

[33] M. Akhtar, M. Hanif, and N. Ranjha, "Methods of synthesis of hydrogels … A Review," *Saudi Pharmaceutical Journal*, vol. 13, Mar. 2015, doi: 10.1016/j.jsps.2015.03.022.

[34] H. Janik and M. Marzec, "A review: Fabrication of porous polyurethane scaffolds," *Materials Science and Engineering: C*, vol. 48, pp. 586–591, Mar. 2015, doi: 10.1016/j.msec.2014.12.037.

[35] V. M. Gun'ko, I. N. Savina, and S. V. Mikhalovsky, "Cryogels: Morphological, structural and adsorption characterisation," *Advances in Colloid and Interface Science*, vol. 187–188, pp. 1–46, Jan. 2013, doi: 10.1016/j.cis.2012.11.001.

[36] A. Memic *et al.*, "Latest Advances in Cryogel Technology for Biomedical Applications," *Advanced Therapeutics*, vol. 2, no. 4, p. 1800114, 2019, doi: 10.1002/adtp.201800114.

[37] V. I. Lozinsky, "Cryostructuring of Polymeric Systems. 55. Retrospective View on the More than 40 Years of Studies Performed in the

A.N.Nesmeyanov Institute of Organoelement Compounds with Respect of the Cryostructuring Processes in Polymeric Systems," *Gels*, vol. 6, no. 3, p. E29, Sep. 2020, doi: 10.3390/gels6030029.

[38] P. A. Shiekh, S. M. Andrabi, A. Singh, S. Majumder, and A. Kumar, "Designing cryogels through cryostructuring of polymeric matrices for biomedical applications," *European Polymer Journal*, vol. 144, p. 110234, Feb. 2021, doi: 10.1016/j.eurpolymj.2020.110234.

[39] I. N. Savina, G. C. Ingavle, A. B. Cundy, and S. V. Mikhalovsky, "A simple method for the production of large volume 3D macroporous hydrogels for advanced biotechnological, medical and environmental applications," *Sci Rep*, vol. 6, no. 1, Art. no. 1, Feb. 2016, doi: 10.1038/srep21154.

[40] S. Bencherif, T. Braschler, and P. Renaud, "Advances in the design of macroporous polymer scaffolds for potential applications in dentistry," *Journal of periodontal & implant science*, vol. 43, pp. 251–261, Dec. 2013, doi: 10.5051/jpis.2013.43.6.251.

[41] L. J. Eggermont, Z. J. Rogers, T. Colombani, A. Memic, and S. A. Bencherif, "Injectable Cryogels for Biomedical Applications," *Trends in Biotechnology*, vol. 38, no. 4, pp. 418–431, Apr. 2020, doi: 10.1016/j.tibtech.2019.09.008.

[42] M. Razavi, Y. Qiao, and A. S. Thakor, "Three-dimensional cryogels for biomedical applications," *Journal of Biomedical Materials Research Part A*, vol. 107, no. 12, pp. 2736–2755, 2019, doi: 10.1002/jbm.a.36777.

[43] T. Vishnoi and A. Kumar, "Conducting cryogel scaffold as a potential biomaterial for cell stimulation and proliferation," *J Mater Sci Mater Med*, vol. 24, no. 2, pp. 447–459, Feb. 2013, doi: 10.1007/s10856-012-4795-z.

[44] S. A. Bencherif *et al.*, "Injectable preformed scaffolds with shape-memory properties," *Proc Natl Acad Sci U S A*, vol. 109, no. 48, pp. 19590–19595, Nov. 2012, doi: 10.1073/pnas.1211516109.

[45] V. I. Lozinsky, I. Yu. Galaev, F. M. Plieva, I. N. Savina, H. Jungvid, and B. Mattiasson, "Polymeric cryogels as promising materials of biotechnological interest," *Trends in Biotechnology*, vol. 21, no. 10, pp. 445–451, Oct. 2003, doi: 10.1016/j.tibtech.2003.08.002.

[46] A. Kumar, R. Mishra, Y. Reinwald, and S. Bhat, "Cryogels: Freezing unveiled by thawing," *Materials Today*, vol. 13, no. 11, pp. 42–44, Nov. 2010, doi: 10.1016/S1369-7021(10)70202-9.

[47] W. C. Reygaert, "An overview of the antimicrobial resistance mechanisms of bacteria," *AIMS Microbiol*, vol. 4, no. 3, pp. 482–501, Jun. 2018, doi: 10.3934/microbiol.2018.3.482.

[48] B. Li and T. J. Webster, "Bacteria antibiotic resistance: New challenges and opportunities for implant-associated orthopedic infections," *Journal of Orthopaedic Research*, vol. 36, no. 1, pp. 22–32, 2018, doi: 10.1002/jor.23656.

[49] Y. Pan, Q. Xia, and H. Xiao, "Cationic Polymers with Tailored Structures for Rendering Polysaccharide-Based Materials Antimicrobial: An Overview,"

Polymers, vol. 11, no. 8, Art. no. 8, Aug. 2019, doi: 10.3390/polym11081283.

[50] A. M. Carmona-Ribeiro and L. D. De Melo Carrasco, "Cationic Antimicrobial Polymers and Their Assemblies," *International Journal of Molecular Sciences*, vol. 14, no. 5, Art. no. 5, May 2013, doi: 10.3390/ijms14059906.

[51] A. S. Veiga and J. P. Schneider, "Antimicrobial hydrogels for the treatment of infection," *Biopolymers*, vol. 100, no. 6, p. 637, 2013.

[52] Y. Huang, L. Bai, Y. Yang, Z. Yin, and B. Guo, "Biodegradable gelatin/silver nanoparticle composite cryogel with excellent antibacterial and antibiofilm activity and hemostasis for Pseudomonas aeruginosa-infected burn wound healing," *Journal of Colloid and Interface Science*, vol. 608, pp. 2278–2289, Feb. 2022, doi: 10.1016/j.jcis.2021.10.131.

[53] T. Abdullah, T. Colombani, T. Alade, S. A. Bencherif, and A. Memić, "Injectable Lignin-co-Gelatin Cryogels with Antioxidant and Antibacterial Properties for Biomedical Applications," *Biomacromolecules*, vol. 22, no. 10, pp. 4110–4121, Oct. 2021, doi: 10.1021/acs.biomac.1c00575.

[54] L. Yao *et al.*, "A shape memory and antibacterial cryogel with rapid hemostasis for noncompressible hemorrhage and wound healing," *Chemical Engineering Journal*, vol. 428, p. 131005, Jan. 2022, doi: 10.1016/j.cej.2021.131005.

[55] Y. Xue and H. Xiao, "Antibacterial/Antiviral Property and Mechanism of Dual-Functional Quaternized Pyridinium-type Copolymer," *Polymers*, vol. 7, no. 11, Art. no. 11, Nov. 2015, doi: 10.3390/polym7111514.

[56] J. M. Vaz, D. Pezzoli, P. Chevallier, C. S. Campelo, G. Candiani, and D. Mantovani, "Antibacterial Coatings Based on Chitosan for Pharmaceutical and Biomedical Applications," *Current Pharmaceutical Design*, vol. 24, no. 8, pp. 866–885, Mar. 2018, doi: 10.2174/1381612824666180219143900.

[57] Z.-X. Peng, L. Wang, L. Du, S.-R. Guo, X.-Q. Wang, and T.-T. Tang, "Adjustment of the antibacterial activity and biocompatibility of hydroxypropyltrimethyl ammonium chloride chitosan by varying the degree of substitution of quaternary ammonium," *Carbohydrate Polymers*, vol. 81, no. 2, pp. 275–283, Jun. 2010, doi: 10.1016/j.carbpol.2010.02.008.

[58] M. Li, Z. Zhang, Y. Liang, J. He, and B. Guo, "Multifunctional Tissue-Adhesive Cryogel Wound Dressing for Rapid Nonpressing Surface Hemorrhage and Wound Repair," *ACS Appl. Mater. Interfaces*, vol. 12, no. 32, pp. 35856–35872, Aug. 2020, doi: 10.1021/acsami.0c08285.

[59] H. Tan, Z. Peng, Q. Li, X. Xu, S. Guo, and T. Tang, "The use of quaternised chitosan-loaded PMMA to inhibit biofilm formation and downregulate the virulence-associated gene expression of antibiotic-resistant staphylococcus," *Biomaterials*, vol. 33, no. 2, pp. 365–377, Jan. 2012, doi: 10.1016/j.biomaterials.2011.09.084.

[60] B. C. Allison, B. M. Applegate, and J. P. Youngblood, "Hemocompatibility of Hydrophilic Antimicrobial Copolymers of Alkylated 4-Vinylpyridine,"

Biomacromolecules, vol. 8, no. 10, pp. 2995–2999, Oct. 2007, doi: 10.1021/bm7004627.

[61] D. Berillo, A. Al-Jwaid, and J. Caplin, "Polymeric Materials Used for Immobilisation of Bacteria for the Bioremediation of Contaminants in Water," *Polymers*, vol. 13, no. 7, Art. no. 7, Jan. 2021, doi: 10.3390/polym13071073.

[62] D. A. Berillo, J. L. Caplin, A. B. Cundy, and I. N. Savina, "A cryogel-based bioreactor for water treatment applications," *Water Research*, vol. 153, pp. 324–334, Apr. 2019, doi: 10.1016/j.watres.2019.01.028.

[63] L. Hao *et al.*, "Preparation of immobilized ε-polylysine PET nonwoven fabrics and antibacterial activity evaluation," *J. Wuhan Univ. Technol.-Mat. Sci. Edit.*, vol. 26, no. 4, pp. 675–680, Aug. 2011, doi: 10.1007/s11595-011-0290-5.

[64] D. Demir, S. Özdemir, M. S. Yalçın, and N. Bölgen, "Chitosan cryogel microspheres decorated with silver nanoparticles as injectable and antimicrobial scaffolds," *International Journal of Polymeric Materials and Polymeric Biomaterials*, vol. 69, no. 14, pp. 919–927, Sep. 2020, doi: 10.1080/00914037.2019.1631823.

[65] E. Montanari *et al.*, "Chasing bacteria within the cells using levofloxacin-loaded hyaluronic acid nanohydrogels," *Eur J Pharm Biopharm*, vol. 87, no. 3, pp. 518–523, Aug. 2014, doi: 10.1016/j.ejpb.2014.03.003.

[66] B. Ari, S. Demirci, R. S. Ayyala, B. Salih, and N. Sahiner, "Superporous poly(β-Cyclodextrin) cryogels as promising materials for simultaneous delivery of both hydrophilic and hydrophobic drugs," *European Polymer Journal*, vol. 176, p. 111399, Aug. 2022, doi: 10.1016/j.eurpolymj.2022.111399.

[67] D. Pamfil, E. Butnaru, and C. Vasile, "Poly (vinyl alcohol)/chitosan cryogels as PH responsive ciprofloxacin carriers," *J Polym Res*, vol. 23, no. 8, p. 146, Jul. 2016, doi: 10.1007/s10965-016-1042-1.

[68] L. P. Bagri, J. Bajpai, and A. K. Bajpai, "Evaluation of starch based cryogels as potential biomaterials for controlled release of antibiotic drugs," *Bull Mater Sci*, vol. 34, no. 7, pp. 1739–1748, Dec. 2011, doi: 10.1007/s12034-011-0385-9.

[69] G. Pandey *et al.*, "Dual functioning microspheres embedded crosslinked gelatin cryogels for therapeutic intervention in osteomyelitis and associated bone loss," *European Journal of Pharmaceutical Sciences*, vol. 91, pp. 105–113, Aug. 2016, doi: 10.1016/j.ejps.2016.06.008.

[70] A. Chaturvedi, A. K. Bajpai, J. Bajpai, and A. Sharma, "Antimicrobial poly(vinyl alcohol) cryogel–copper nanocomposites for possible applications in biomedical fields," *Designed Monomers and Polymers*, vol. 18, no. 4, pp. 385–400, May 2015, doi: 10.1080/15685551.2015.1012628.

[71] Y. Huang, L. Bai, Y. Yang, Z. Yin, and B. Guo, "Biodegradable gelatin/silver nanoparticle composite cryogel with excellent antibacterial and antibiofilm activity and hemostasis for Pseudomonas aeruginosa-infected burn wound

healing," *Journal of Colloid and Interface Science*, vol. 608, pp. 2278–2289, Feb. 2022, doi: 10.1016/j.jcis.2021.10.131.

[72] D. Berillo, "Gold nanoparticles incorporated into cryogel walls for efficient nitrophenol conversion," *Journal of Cleaner Production*, vol. 247, p. 119089, Feb. 2020, doi: 10.1016/j.jclepro.2019.119089.

[73] G. Nam, S. Rangasamy, B. Purushothaman, and J. M. Song, "The Application of Bactericidal Silver Nanoparticles in Wound Treatment," *Nanomaterials and Nanotechnology*, vol. 5, no. Godište 2015, pp. 5–23, Jan. 2015, doi: 10.5772/60918.

[74] D. Kharaghani *et al.*, "Development of antibacterial contact lenses containing metallic nanoparticles," *Polymer Testing*, vol. 79, p. 106034, Oct. 2019, doi: 10.1016/j.polymertesting.2019.106034.

[75] A. Muniyan, K. Ravi, U. Mohan, and R. Panchamoorthy, "Characterization and in vitro antibacterial activity of saponin-conjugated silver nanoparticles against bacteria that cause burn wound infection," *World J Microbiol Biotechnol*, vol. 33, no. 7, p. 147, Jun. 2017, doi: 10.1007/s11274-017-2309-3.

[76] K. S. U. Suganya *et al.*, "Size controlled biogenic silver nanoparticles as antibacterial agent against isolates from HIV infected patients," *Spectrochimica Acta Part A: Molecular and Biomolecular Spectroscopy*, vol. 144, pp. 266–272, Jun. 2015, doi: 10.1016/j.saa.2015.02.074.

[77] N. Xu *et al.*, "Multifunctional chitosan/gelatin@tannic acid cryogels decorated with in situ reduced silver nanoparticles for wound healing," *Burns & Trauma*, vol. 10, p. tkac019, Jan. 2022, doi: 10.1093/burnst/tkac019.

[78] A. Haleem, S.-Q. Chen, M. Ullah, M. Siddiq, and W.-D. He, "Highly porous cryogels loaded with bimetallic nanoparticles as an efficient antimicrobial agent and catalyst for rapid reduction of water-soluble organic contaminants," *Journal of Environmental Chemical Engineering*, vol. 9, no. 6, p. 106510, Dec. 2021, doi: 10.1016/j.jece.2021.106510.

[79] M. S. Kadayifci *et al.*, "Core-crosslinking as a pathway to develop inherently antibacterial polymeric micelles," *Journal of Applied Polymer Science*, vol. 137, no. 8, p. 48393, 2020.

[80] O. I. Parisi, L. Scrivano, M. S. Sinicropi, and F. Puoci, "Polymeric nanoparticle constructs as devices for antibacterial therapy," *Current Opinion in Pharmacology*, vol. 36, pp. 72–77, Oct. 2017, doi: 10.1016/j.coph.2017.08.004.

[81] I. Qayoom, E. Srivastava, and A. Kumar, "Anti-infective composite cryogel scaffold treats osteomyelitis and augments bone healing in rat femoral condyle," *Biomaterials Advances*, vol. 142, p. 213133, Nov. 2022, doi: 10.1016/j.bioadv.2022.213133.

[82] R. Kumar Saini, L. Prasad Bagri, and A. K. Bajpai, "Nano-silver hydroxyapatite based antibacterial 3D scaffolds of gelatin/alginate/poly (vinyl alcohol) for bone tissue engineering applications," *Colloids and*

Surfaces B: Biointerfaces, vol. 177, pp. 211–218, May 2019, doi: 10.1016/j.colsurfb.2019.01.064.

[83] P. Li *et al.*, "A resilient and flexible chitosan/silk cryogel incorporated Ag/Sr co-doped nanoscale hydroxyapatite for osteoinductivity and antibacterial properties," *J. Mater. Chem. B*, vol. 6, no. 45, pp. 7427–7438, Nov. 2018, doi: 10.1039/C8TB01672K.

[84] D. S. Kauvar, R. Lefering, and C. E. Wade, "Impact of Hemorrhage on Trauma Outcome: An Overview of Epidemiology, Clinical Presentations, and Therapeutic Considerations," *Journal of Trauma and Acute Care Surgery*, vol. 60, no. 6, p. S3, Jun. 2006, doi: 10.1097/01.ta.0000199961.02677.19.

[85] N. Sahiner, S. Yildiz, and H. Al-Lohedan, "The resourcefulness of p(4-VP) cryogels as template for in situ nanoparticle preparation of various metals and their use in H2 production, nitro compound reduction and dye degradation," *Applied Catalysis B: Environmental*, vol. 166–167, pp. 145–154, May 2015, doi: 10.1016/j.apcatb.2014.11.027.

[86] F. Lowy, "Bacterial Classification, Structure and Function," p. 8.

[87] A. Helmenstine, "Prokaryotic vs Eukaryotic Cells - Similarities and Differences," *Science Notes and Projects*, Mar. 15, 2022. https://sciencenotes.org/prokaryotic-vs-eukaryotic-similarities-and-differences/ (accessed Nov. 12, 2022).

[88] T. Y. Liu *et al.*, "Differentiation of bacteria cell wall using Raman scattering enhanced by nanoparticle array," *J Nanosci Nanotechnol*, vol. 12, no. 6, pp. 5004–5008, Jun. 2012, doi: 10.1166/jnn.2012.4941.

[89] K. Dufresne and C. Paradis-Bleau, "Biology and Assembly of the Bacterial Envelope," in *Prokaryotic Systems Biology*, P. Krogan Nevan J. and P. Babu Mohan, Eds. Cham: Springer International Publishing, 2015, pp. 41–76. doi: 10.1007/978-3-319-23603-2_3.

[90] D. T. K. Haneef Jazir, "10 Differences between Cell wall of Gram positive and Gram negative Bacteria," *Major Differences*. https://www.majordifferences.com/2018/06/difference-between-cell-wall-of-gram.html (accessed Nov. 28, 2022).

[91] A. L. Koch, *The bacteria: their origin, structure, function and antibiosis*. Dordrecht: Springer, 2006.

[92] P. Cardoso *et al.*, "Molecular engineering of antimicrobial peptides: microbial targets, peptide motifs and translation opportunities," *Biophys Rev*, vol. 13, no. 1, pp. 35–69, Feb. 2021, doi: 10.1007/s12551-021-00784-y.

[93] "Multi Resistant Bacteria & Phospholipids - Antibiotics Research and Lipid Analysis," *Lipotype GmbH*. https://www.lipotype.com/lipidomics-applications/lipidomics-of-multi-resistant-bacteria/ (accessed Nov. 19, 2022).

[94] M. Topuzogullari, “Microwave assisted quaternization of poly(4-vinylpyridine) with 1-bromohexane,” *J Polym Res*, vol. 25, no. 8, p. 188, Jul. 2018, doi: 10.1007/s10965-018-1581-8.

[95] Z. Olcer, M. M. Ozmen, Z. M. Sahin, F. Yilmaz, and A. Tanriseven, “Highly Efficient Method Towards in Situ Immobilization of Invertase Using Cryogelation,” *Appl Biochem Biotechnol*, vol. 171, no. 8, pp. 2142–2152, Dec. 2013, doi: 10.1007/s12010-013-0507-5.

[96] “Standard Test Method for Determining the Antimicrobial Activity of Immobilized Antimicrobial Agents Under Dynamic Contact Conditions.” https://www.astm.org/e2149-13.html (accessed Nov. 23, 2022).

[97] A. Kruk, A. Gadomska-Gajadhur, J. Dulnik, and P. Ruśkowski, “The influence of the molecular weight of polymer on the morphology, functional properties and L929 fibroblasts growth on polylactide membranes for tissue engineering,” *International Journal of Polymeric Materials and Polymeric Biomaterials*, vol. 71, no. 1, pp. 45–57, Jan. 2022, doi: 10.1080/00914037.2020.1798440.

[98] S. Hou, Y. Liu, F. Feng, J. Zhou, X. Feng, and Y. Fan, “Polysaccharide-Peptide Cryogels for Multidrug-Resistant-Bacteria Infected Wound Healing and Hemostasis,” *Advanced Healthcare Materials*, vol. 9, no. 3, p. 1901041, 2020, doi: 10.1002/adhm.201901041.

[99] X. Zhao, B. Guo, H. Wu, Y. Liang, and P. X. Ma, “Injectable antibacterial conductive nanocomposite cryogels with rapid shape recovery for noncompressible hemorrhage and wound healing,” *Nat Commun*, vol. 9, no. 1, Art. no. 1, Jul. 2018, doi: 10.1038/s41467-018-04998-9.

[100] G. Kulkarni, P. Guha Ray, P. K. Byram, M. Kaushal, S. Dhara, and S. Das, “Tailorable hydrogel of gelatin with silk fibroin and its activation/crosslinking for enhanced proliferation of fibroblast cells,” *Int J Biol Macromol*, vol. 164, pp. 4073–4083, Dec. 2020, doi: 10.1016/j.ijbiomac.2020.09.016.

[101] M. Topuzogullari, V. Bulmus, E. Dalgakiran, and S. Dincer, “pH- and temperature-responsive amphiphilic diblock copolymers of 4-vinylpyridine and oligoethyleneglycol methacrylate synthesized by RAFT polymerization,” *Polymer*, vol. 55, no. 2, pp. 525–534, Jan. 2014, doi: 10.1016/j.polymer.2013.12.040.

[102] M. Topuzogullari, Y. B. Elalmis, and S. D. Isoglu, “Thermo-Responsive Complexes of c-Myc Antisense Oligonucleotide with Block Copolymer of Poly(OEGMA) and Quaternized Poly(4-Vinylpyridine),” *Macromolecular Bioscience*, vol. 17, no. 4, p. 1600263, 2017, doi: 10.1002/mabi.201600263.

[103] Y. Elsayed and C. Lekakou, “2 - Designing and modeling pore size distribution in tissue scaffolds,” in *Characterisation and Design of Tissue Scaffolds*, P. Tomlins, Ed. Woodhead Publishing, 2016, pp. 23–43. doi: 10.1016/B978-1-78242-087-3.00002-X.

[104] E. S. Dragan, M. M. Lazar, M. V. Dinu, and F. Doroftei, “Macroporous composite IPN hydrogels based on poly(acrylamide) and chitosan with tuned swelling and sorption of cationic dyes,” *Chemical Engineering Journal*, vol. 204–206, pp. 198–209, Sep. 2012, doi: 10.1016/j.cej.2012.07.126.

[105] S. Demirci and N. Sahiner, “Superporous neutral, anionic, and cationic cryogel reactors to improved enzymatic activity and stability of α-Glucosidase enzyme via entrapment method,” *Chemical Engineering Journal*, vol. 409, p. 128233, Apr. 2021, doi: 10.1016/j.cej.2020.128233.

[106] N. Sahiner, S. Yildiz, M. Sahiner, Z. A. Issa, and H. Al-Lohedan, “Macroporous cryogel metal nanoparticle composites for H2 generation from NaBH4 hydrolysis in seawater,” *Applied Surface Science*, vol. 354, pp. 388–396, Nov. 2015, doi: 10.1016/j.apsusc.2015.04.183.

[107] A. Naskar, S. Lee, Y. Lee, S. Kim, and K. Kim, “A New Nano-Platform of Erythromycin Combined with Ag Nano-Particle ZnO Nano-Structure against Methicillin-Resistant Staphylococcus aureus,” *Pharmaceutics*, vol. 12, no. 9, Art. no. 9, Sep. 2020, doi: 10.3390/pharmaceutics12090841.

[108] A. Ray Mohapatra, A. Harikrishnan, D. Lakshmanan, and K. Jeevaratnam, “Targeting Staphylococcus aureus and its biofilms with novel antibacterial compounds produced by Lactiplantibacillus plantarum SJ33,” *Arch Microbiol*, vol. 204, no. 1, p. 20, Dec. 2021, doi: 10.1007/s00203-021-02630-x.

[109] T. R. Stratton, J. L. Rickus, and J. P. Youngblood, “In Vitro Biocompatibility Studies of Antibacterial Quaternary Polymers,” *Biomacromolecules*, vol. 10, no. 9, pp. 2550–2555, Sep. 2009, doi: 10.1021/bm9005003.

[110] M. G. Drozdova *et al.*, “Macroporous modified poly (vinyl alcohol) hydrogels with charged groups for tissue engineering: Preparation and in vitro evaluation,” *Materials Science and Engineering: C*, vol. 75, pp. 1075–1082, Jun. 2017, doi: 10.1016/j.msec.2017.03.017.

[111] O. Janoušková, M. Přádný, M. Vetrík, E. C. Krumbholcová, J. Michálek, and M. D. Smrčková, “Biomimetic modification of dual porosity poly(2-hydroxyethyl methacrylate) hydrogel scaffolds—porosity and stem cell growth evaluation,” *Biomed. Mater.*, vol. 14, no. 5, p. 055004, Jul. 2019, doi: 10.1088/1748-605X/ab2856.

[112] M. G. Drozdova *et al.*, “Macroporous modified poly (vinyl alcohol) hydrogels with charged groups for tissue engineering: Preparation and in vitro evaluation,” *Materials Science and Engineering: C*, vol. 75, pp. 1075–1082, Jun. 2017, doi: 10.1016/j.msec.2017.03.017.

PUBLICATIONS FROM THE THESIS

Conference Papers

1. Daaboul M., Topuzoğulları M., Özmen M.M., "Polimerik Nanopartikül Gömülü Katyonik Kriyojellerin Sentezi ve Karakterizasyonu", The 8th Polymer Science and Technology Congress with International Participitation, Malatya, Turkey, June 20-23, 2022.

Projects

1. "Kendiliğinden Antibakteriyel Polimerik Malzemelerin Geliştirilmesi", The Scientific Research Projects Coordination Unit of Yildiz Technical University, Project No: FCD-2022-4900, Project Manager: Assoc. Prof. Dr. Murat Topuzoğulları, 2022-2024.